

17.63 and 18.14 Mev States in Be<sup>8</sup>

Thesis by

David A. Liberman

In Partial Fulfillment of the Requirements

for the Degree of

Doctor of Philosophy

California Institute of Technology

Pasadena, California

1955

## ACKNOWLEDGEMENTS

I wish to thank Professor R.F. Christy, who suggested this problem, for his patient help and guidance in seeing it through to completion. I am also indebted to Dr. W.D. Warters, Dr. A.A. Kraus, and Professor W.A. Fowler for numerous discussions of the experimental data.

Part of the work described in this thesis was done during the academic year 1952 - 1953 when I held a Dow Chemical Company fellowship. I should like to thank the Physics Department for appointing me to this fellowship and the Dow Chemical Company for its financial support.

## ABSTRACT

The experimental data relating to the 17.63 and 18.14 Mev states in  $\text{Be}^8$  is analyzed. It is shown that all available measurements are consistent with the assumption that both states have  $J = 1^+$ . Since these states are obtained by bombarding  $\text{Li}^7$  ( $J = 3/2^-$ ) with protons, they must be formed principally by p-wave protons. Ordinarily  $\cos^2\theta$  terms would be expected in angular distributions for reactions involving these states, but they are not observed. From this it is concluded that a certain value of the channel spin ratio -  $\alpha_1^2/\alpha_2^2 = 1/5$  - is required. It is then shown that this value may be obtained on the assumption of an independent particle model with either jj or LS coupling. The particle and radiation widths are computed for these states using both LS and jj coupling schemes, and the results are found to be in order-of-magnitude agreement with experiment.

## TABLE OF CONTENTS

Part	Title	Page
I.	INTRODUCTION	1
II.	DISCUSSION OF EXPERIMENTAL DATA AND THE ASSIGNMENT OF QUANTUM NUMBERS	2
	A. 17.63 Mev Level	2
	1. Gamma Radiation	2
	2. Elastic Scattering	12
	B. 18.14 Mev Level	16
	1. Gamma Radiation	17
	2. Elastic Scattering	20
	3. Inelastic Scattering	29
	C. Phase Shift Analysis	30
III.	INDEPENDENT PARTICLE MODEL WAVE FUNCTIONS AND LEVEL PARAMETERS	40
	A. Wave Functions for jj Coupling Model	41
	1. $J = 3/2^-$ Wave Functions for $\text{Li}^7$	45
	2. $J = 1/2^-$ Wave Functions for $\text{Li}^7$	49
	3. $J = 1^+$ Wave Functions for $\text{Be}^8$	50
	4. $J = 0^+$ Wave Functions for $\text{Be}^8$	57
	5. Channel Spin Wave Functions	58
	B. Wave Functions for LS Coupling Model	60
	1. $J = 3/2^-$ Wave Functions for $\text{Li}^7$	62
	2. $J = 1/2^-$ Wave Functions for $\text{Li}^7$	69
	3. $J = 1^+$ Wave Functions for $\text{Be}^8$	71

4.	$J = 0^+$ Wave Functions for $\text{Be}^8$	74
5.	Channel Spin Wave Functions	76
C.	Radiative Decay Widths	76
D.	Particle Emission Widths	80
E.	Discussion of Level Parameters	85
	REFERENCES	89

## I. INTRODUCTION

The study of the energy levels of nuclei has a dual aim : on one hand there is the hope that it may give clues as to the exact nature of nuclear forces, and on the other hand that it will lead to a systematics of nuclei in analogy to our knowledge of atoms. Some success may be claimed for this program on both scores. The charge symmetric nature of nuclear forces serves as an example of the former and the Mayer - Jensen shell model of the latter.

The independent particle picture of the atomic nucleus - of which the Mayer - Jensen shell model is an important example - is a direct copy from conventional atomic physics. There it has the advantage of a sound theoretical basis and a great deal of experimental confirmation. The strong, short range nature of nuclear forces leads one to expect a much higher degree of correlation in the motion of nucleons in the nucleus than is suggested by the independent particle picture. Nonetheless the independent particle picture has been used with considerable success of late in accounting for many observed properties of nuclei : spins, magnetic moments, energy levels, etc.

This thesis is a report on an attempt at applying some of the ideas of the independent particle picture to two states in  $\text{Be}^8$  which are excited by bombarding  $\text{Li}^7$  with protons. The first part consists in a careful analysis of the experimental data which establishes with a fairly high degree of probability that both of these states have spin one and are formed from p-wave protons. Also it is shown that in both cases the differential cross sections for scattering

and radiative capture has no or very little dependence on  $P_2(\cos \theta)$  contrary to what one would off hand expect in the case of p-waves.

In the second part of this thesis independent particle wave functions are developed according to the jj and LS coupling models. For certain wave functions in either scheme it is shown that the curious absence of the  $P_2(\cos \theta)$  term is predicted. Using these same wave functions, other level parameters are also computed (particle widths and radiation probabilities) and these are compared with experiment in the hope that all of the data connected with a given energy level may be accounted for by a single wave function. Only very partial success can be claimed for correlating all of the data by this attempt.

## II. DISCUSSION OF THE EXPERIMENTAL DATA AND THE ASSIGNMENT OF QUANTUM NUMBERS

### A. 17.63 Mev Level

Two types of experimental data are available relating to the 17.63 Mev state in  $\text{Be}^8$ . One is the elastic scattering cross section for protons on  $\text{Li}^7$  known as a function of energy and angle, and the other is the cross section for the radiative capture of protons by  $\text{Li}^7$  which is also known at a variety of bombarding energies for the proton and several angles for the emitted gamma ray. In the following it will be established that both types of information are consistent with a certain choice of spin, parity, and channel spin ratio for the excited state in  $\text{Be}^8$ . Other possibilities will be considered and rejected as most improbable.

#### A.1. Gamma Radiation<sup>(1,2)</sup>

The most striking datum at our disposal is the angular distribution of gamma rays obtained at the peak of the resonance. It is very nearly isotropic : Devons and Hine give as the angular distribution at this energy  $1 + 0.05 \cos \theta$ .

The most common explanations for isotropic angular distributions are that the resonant state is formed by an s-wave or that the resonant state has a total angular momentum of 0 or 1/2. The latter possibility may be ruled out immediately, for the ground state of  $\text{Be}^8$  has  $J = 0$  so that the assumption of  $J = 0$  for the



excited state means that gamma radiation would be strictly forbidden. It has been observed in several different experiments<sup>(1,3,4)</sup> that most of the resonant radiation leaves  $\text{Be}^8$  in the ground state and not in the lower excited states although such transitions do occur.

Devons and Hine<sup>(2)</sup> analyzed their data on the assumption that the resonance was due to an s-wave, so it is not necessary to explore this possibility in detail here. It will suffice to set forth the arguments against this assumption and those in favour of assigning this state to p-waves.

The observed gamma radiation width of the 17.63 Mev state in  $\text{Be}^8$  is

$$\Gamma_{\gamma} = \frac{(2i + 1)(2I + 1)}{2J + 1} \cdot 9.4 = \frac{8}{2J + 1} \cdot 9.4 \text{ ev}$$

where  $i = 1/2$  is the spin of the proton,  $I = 3/2$  is the spin of  $\text{Li}^7$  and  $J$  is the spin of  $\text{Be}^8$  in the compound state, the value of which is unknown at this early stage of the analysis. For the present purposes we may think of the gamma width as having a value of 10 or 20 ev. This value may then be compared with approximate theoretical predictions such as those of Weisskopf<sup>(5)</sup> which may be taken as a rough upper limit on what may be expected.

When s-wave protons bombard  $\text{Li}^7$ , compound states with  $J = 1^-$  and  $J = 2^-$  may be formed. In the first case the compound nucleus may decay by electric dipole radiation and in the second case by magnetic quadrupole radiation to the  $J = 0^+$  ground state of  $\text{Be}^8$ . Weisskopf's formulas give  $\Gamma_{\gamma} = 2000$  ev for the case of electric dipole radiation and  $\Gamma_{\gamma} = 1/4$  ev in the case of magnetic quadrupole radiation. On the basis of these two figures magnetic

quadrupole radiation can easily be ruled out (and hence the  $J = 2^-$  state) while the possibility that the resonant radiation is electric dipole still remains. The decision against assuming the resonant state as  $J = 2^-$  is further supported by noting that a  $J = 2^-$  state can decay to the  $J = 2^+$  first excited state of  $\text{Be}^8$  by electric dipole radiation. This means that this mode of decay should be much favoured over decay to the ground state, but, as noted above, the contrary is the case.

The experiments, it was mentioned above, show an angular distribution at the peak of the resonance with a small but definite  $\cos\theta$  term. This must be due to interference of the resonant state with one or more states of opposite parity. If the resonance is formed by an s-wave, the most likely interfering states are those formed by p-waves. From p-waves states with  $J = 0^+, 1^+, 2^+$  and  $3^+$  can be formed, but it is to be expected that the  $J = 1^+$  states will contribute most strongly in the radiation to the ground state of  $\text{Be}^8$ . (It is assumed here that none of these states are resonant as there is no evidence for that in the experimental cross sections.)

The transition from  $J = 1^+$  to  $J = 0^+$  goes by magnetic dipole radiation. The cross section for this can be estimated using the formulas in the book of Blatt and Weisskopf<sup>(5)</sup> which yield

$$\begin{aligned}\sigma_{\gamma} (M1) &\sim \frac{1}{4} \frac{e^2}{\hbar v} \left(\frac{\omega R}{c}\right)^3 (C_{1kR})^2 \left(\frac{\hbar}{Mc}\right)^2 \\ &= 1.2 \times 10^{-8} \text{ barns.}\end{aligned}$$

( $C_{1kR}$  gives the limiting form of the  $l = 1$  component of the Coulomb wave function near the origin.) If the cross section of the purely

resonant radiation is called  $\sigma_{\gamma R}$ , then the differential cross section including the interference terms can be written

$$\sigma_{\gamma}(\theta) = \frac{1}{4\pi} \left[ \sigma_{\gamma R} \pm 2x \sqrt{\sigma_{\gamma R} \sigma_{\gamma(M1)}} \cos\theta + \sigma_{\gamma(M1)} \right],$$

$$x \ll 1.$$

Since  $\sigma_{\gamma R} \gg \sigma_{\gamma(M1)}$ , the angular distribution will be

$$1 \pm 2x \sqrt{\frac{\sigma_{\gamma(M1)}}{\sigma_{\gamma R}}} \cos\theta.$$

The value of  $\sigma_{\gamma R}$  obtained from experiment<sup>(6)</sup> is  $5.7 \times 10^{-3}$  barns. This value, when combined with the estimate for  $\sigma_{\gamma(M1)}$ , gives the following angular distribution :

$$1 \pm .003x \cos\theta,$$

$$x \ll 1.$$

In this computation the magnitude of the  $\cos\theta$  term has almost certainly been overestimated, and yet it is smaller than the observed value by a factor of more than 15. This means that  $\sigma_{\gamma(M1)}$  is an underestimate on the magnitude of the non-resonant radiation by a factor of over 200.

In a similar manner an estimate can be made of the contribution of a  $J = 2^+$  state through electric quadrupole radiation. The resulting reaction cross section is

$$\sigma_{\gamma(E2)} \sim 6.4 \times 10^{-5} \frac{e^2}{\hbar v} \left(\frac{\omega R}{c}\right)^5 (C_1 kR)^2 R^2$$

$$= 10^{-10} \text{ barns.}$$

This is smaller than the magnetic dipole cross section by a factor of 100 and so will not help us.

The conclusion to draw from the above computations is that the resonant radiation may be explained as electric dipole only at the cost of assuming that the non-resonant radiation is far larger than reasonable theoretical estimates.

Although the assumption that the resonant state is formed by an s-wave is the simplest way of accounting for the observed isotropy of the radiation, it is not the only possibility. As an example, the angular distribution in the case where the compound nucleus is formed by p-waves and has  $J = 1^+$  is

$$1 + \frac{5\alpha_1^2 - \alpha_2^2}{10} P_2(\cos\theta).$$

(Since  $\text{Li}^7$  has a spin  $3/2$  and the proton spin  $1/2$ , the combined system can have "channel spin" 1 or 2. These two channel spins are represented in the wave function of the compound nucleus by relative amplitudes  $\alpha_1$  and  $\alpha_2$  where  $\alpha_1^2 + \alpha_2^2 = 1$ .) By taking  $\alpha_1^2 = 1/6$  and  $\alpha_2^2 = 5/6$  an isotropic angular distribution is obtained. There are many other states where an appropriate choice of the channel spin coefficients will give an isotropic angular distribution. In each such case more or less persuasive arguments can be made against these states, and there remains only the  $J = 1^+$  state with the channel spin ratio  $\alpha_2^2/\alpha_1^2 = 5$  which will now be discussed.

The cross section formulas for resonant radiation from the 17.63 Mev state in  $\text{Be}^8$  to the  $J = 0^+$  ground state and to the  $J = 2^+$  first excited state are, with the non-resonant electric dipole radiation from the  $J = 1^-$  and  $J = 2^-$  states included,

$$\begin{aligned} \sigma_{\gamma_0}(\theta) &= \frac{3}{8k^2} \frac{\Gamma_{\gamma_0}}{\Gamma} \sin^2 \delta \left[ 1 + \frac{5\alpha_1^2 - \alpha_2^2}{10} P_2(\cos \theta) \right] \\ &+ \frac{3}{8k^2} |A|^2 + \frac{3}{4k^2} \sqrt{\frac{3}{2}} \alpha_1 A \sqrt{\frac{\Gamma_{\gamma_0}}{\Gamma}} \sin \delta \cos(\delta + \phi_1) \cos \theta \\ \sigma_{\gamma_2}(\theta) &= \frac{3}{8k^2} \frac{\Gamma_{\gamma_2}}{\Gamma} \sin^2 \delta \left[ 1 + \frac{5\alpha_1^2 - \alpha_2^2}{100} P_2(\cos \theta) \right] \\ &+ \frac{3}{8k^2} |B|^2 + \frac{5}{8k^2} |C|^2 \\ &- \frac{1}{k^2} \sqrt{\frac{\Gamma_{\gamma_2}}{\Gamma}} \sin \delta \cos(\delta + \phi_1) \cos \theta \left[ \frac{3}{8} \sqrt{\frac{3}{2}} \alpha_1 B + \frac{9}{8} \sqrt{\frac{1}{2}} \alpha_2 C \right]. \end{aligned}$$

In this formula A, B, and C are the amplitudes for the non-resonant E1 radiation from the  $J = 1^-$  state (formed by an s-wave) to the  $J = 0^+$  and  $J = 2^+$  states and from the  $J = 2^-$  state to the  $J = 2^+$  state. These quantities are all small compared to the resonant amplitudes and can be estimated theoretically so as to admit comparison with experiment.

Although it is possible to resolve the two gamma rays going to the ground and first excited states of  $\text{Be}^8$ , it is not easy to do so, and most of the data measure both together. Thus what is wanted is the sum of the two cross sections which may be written

$$\sigma_{\gamma}(\theta) = \frac{3}{8k^2} \frac{\Gamma_{\gamma}}{\Gamma} \sin^2 \delta + \frac{3}{4k^2} D \sqrt{\frac{\Gamma_{\gamma}}{\Gamma}} \sin \delta \cos(\delta + \phi_1) \cos \theta$$

where the following simplifications and substitutions have been made:

- 1)  $\alpha_1^2$  and  $\alpha_2^2$  are set equal to 1/6 and 5/6,
- 2)  $\Gamma_\gamma = \Gamma_{\gamma_0} + \Gamma_{\gamma_2}$
- 3) terms in  $A^2$ ,  $B^2$ , and  $C^2$  have been dropped, and
- 4) the terms linear in A, B, and C have been summed together and the total non-resonant amplitude represented by D .

D will be in magnitude about the same size as A, B, and C, and anyone of these may be estimated by the sort of crude computation used above for non-resonant magnetic dipole and electric quadrupole radiation. The result is

$$\frac{4\pi D^2}{k^2} \sim \sigma_{\gamma NR}(E1) \sim \frac{2}{15} \pi R^2 \frac{e^2}{\hbar v} \left(\frac{\omega R}{c}\right)^3 C_0^2$$

$$= 21 \times 10^{-30} \text{ cm}^2 .$$

From this comes an order of magnitude estimate of D :

$$D \sim \pm \frac{1}{6} \times 10^{-2} .$$

Devons and Hine<sup>(1)</sup> present part of their data in the form of the ratio of the intensities measured at two different angles -  $15^\circ$  and  $145^\circ$  - :

$$R = \frac{1 + 2D \sqrt{\frac{\Gamma}{\Gamma_\gamma}} \frac{\cos(\delta + \phi_1)}{\sin \delta} \cos 15^\circ}{1 + 2D \sqrt{\frac{\Gamma}{\Gamma_\gamma}} \frac{\cos(\delta + \phi_1)}{\sin \delta} \cos 145^\circ} .$$

This expression is to be compared with experiment with the understanding that D is the only adjustable constant and that it should not differ too much from the estimated value computed above.

$\Gamma$  and  $\sin \delta$  are taken from the analysis of the elastic scattering and  $\Gamma_\gamma$  from an absolute measurement of the gamma ray yield.<sup>(6)</sup>

In Fig. 1 will be found the experimental values of Devons and Hine and a curve computed from the formula for R using the parameters

$$\Gamma = 14 \text{ kev}, \quad \Gamma_\gamma = 20 \text{ ev}, \quad D = -\frac{1}{10} \times 10^{-2}.$$

The value of D used is seen to be about the same size as that calculated for non-resonant electric dipole radiation. This is in agreement with the assumption that the resonance is formed by p-waves and that the interference term is due to s-waves.

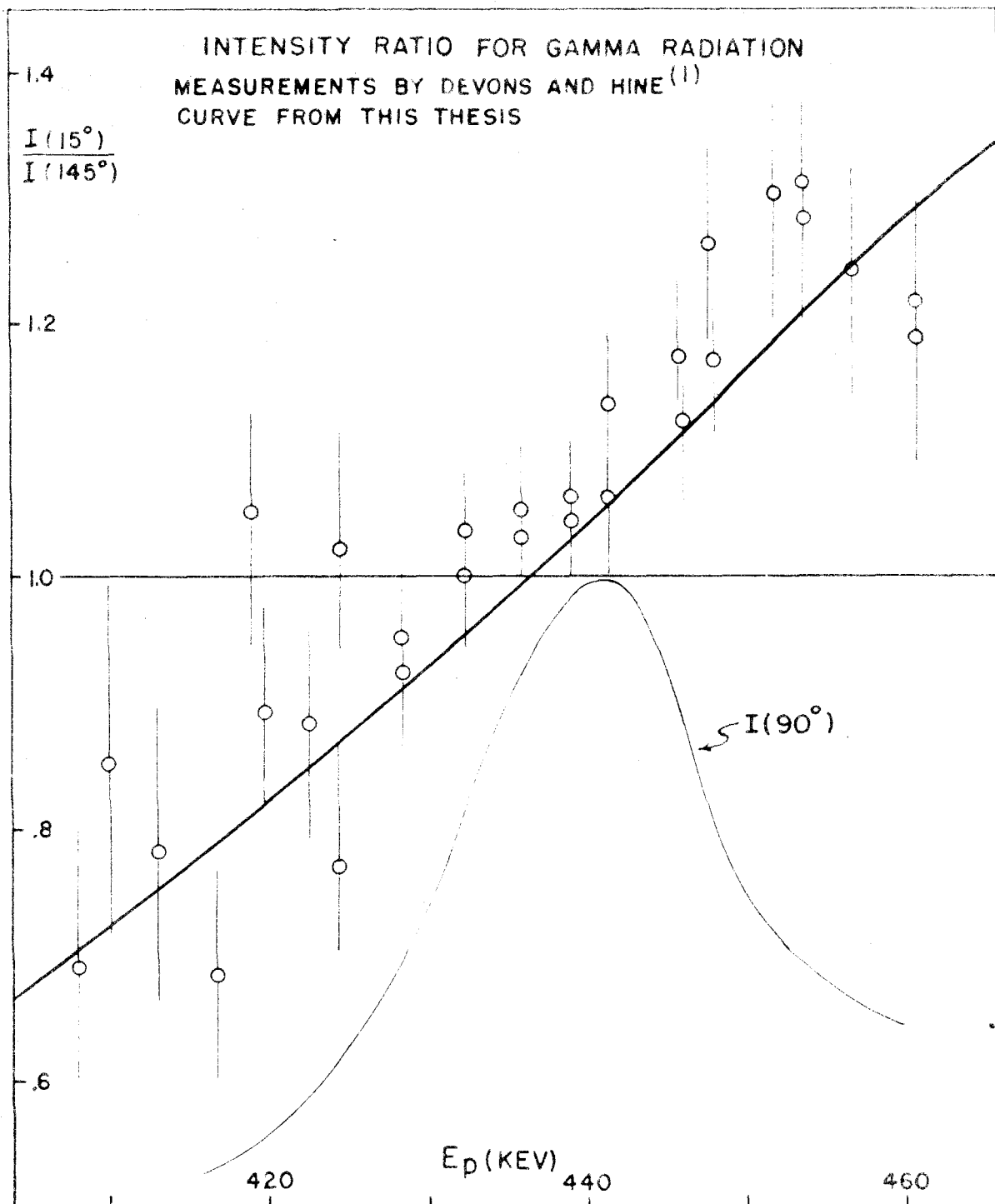


Fig. 1



## A.2. Elastic Scattering

The elastic scattering of protons from  $\text{Li}^7$  was studied by Cohen in his thesis<sup>(7)</sup> where he comes to the correct conclusion that the resonance at 440 kev is formed by p-waves and has  $J = 1^+$ . The cross section formula for this state (given below) has in it an arbitrary parameter which expresses the relative amounts of the two channel spins used in forming this state. Cohen chose a value for this parameter which best fitted the available experimental data. The parameter is the same as that used in describing the gamma ray differential cross sections which means the elastic scattering and gamma ray angular distributions are related.

Cohen chose as his values  $\alpha_1^2 = 0.8, \alpha_2^2 = 0.2$  ( $\alpha_1^2 + \alpha_2^2 = 1$ ) so that the corresponding angular distribution for the gamma rays going to the ground state is

$$\frac{\sigma_{\gamma_0}(\theta)}{\sigma_{\gamma_0}(90^\circ)} = \frac{1 + \frac{5\alpha_1^2 - \alpha_2^2}{10} P_2(\cos\theta)}{1 + \frac{5\alpha_1^2 - \alpha_2^2}{10} \left(-\frac{1}{2}\right)} = 1 + 0.7 \cos^2\theta,$$

and to the first excited state

$$\frac{\sigma_{\gamma_2}(\theta)}{\sigma_{\gamma_2}(90^\circ)} = \frac{1 + \frac{5\alpha_1^2 - \alpha_2^2}{100} P_2(\cos\theta)}{1 + \frac{5\alpha_1^2 - \alpha_2^2}{100} \left(-\frac{1}{2}\right)} = 1 + 0.06 \cos^2\theta.$$

Since, at the peak of the resonance about 3/4 of the transitions

are to the ground state of  $\text{Be}^8(2,3)$ , the net angular distribution would be about

$$\frac{\sigma_{\gamma}(\theta)}{\sigma_{\gamma}(90^{\circ})} = 1 + 0.54 \cos^2 \theta .$$

This prediction is very different from the near isotropy actually observed in the gamma radiation. Devons and Hine<sup>(1)</sup> therefore suggest that the resonant state is in fact formed by s-waves and has  $J = 1^-$ . I have made very elaborate attempts at fitting the observed elastic scattering, assuming the resonant state is that suggested by Devons and Hine and adding varying amounts of p-waves and the  $J = 2^-$  s-wave. The results of these attempts are all very poor; especially when one compares them with those obtained from the correct assignment. To give an account of all these fruitless efforts would serve no good purpose, but one can get a fair idea of the difficulties by plotting on a single graph the experimental angular distribution at the resonant energy and the angular distributions obtained from the phase shift formulas for the two cases :

$$l = 0, J = 1^- \text{ and } l = 1, J = 1^+ .$$

In both of the formulas only one (resonant) state and the Coulomb scattering are considered. The graph (Fig. 2) shows that the p-wave formula is in fair agreement with the data while the s-wave formula shows large deviations from the experimental points especially at backward angles. As stated above, attempts to improve the fit, when an s-wave resonance is assumed, by adding moderate amounts of other phase shifts, do not succeed as the initial fit illustrated in Fig. 2 is so bad.

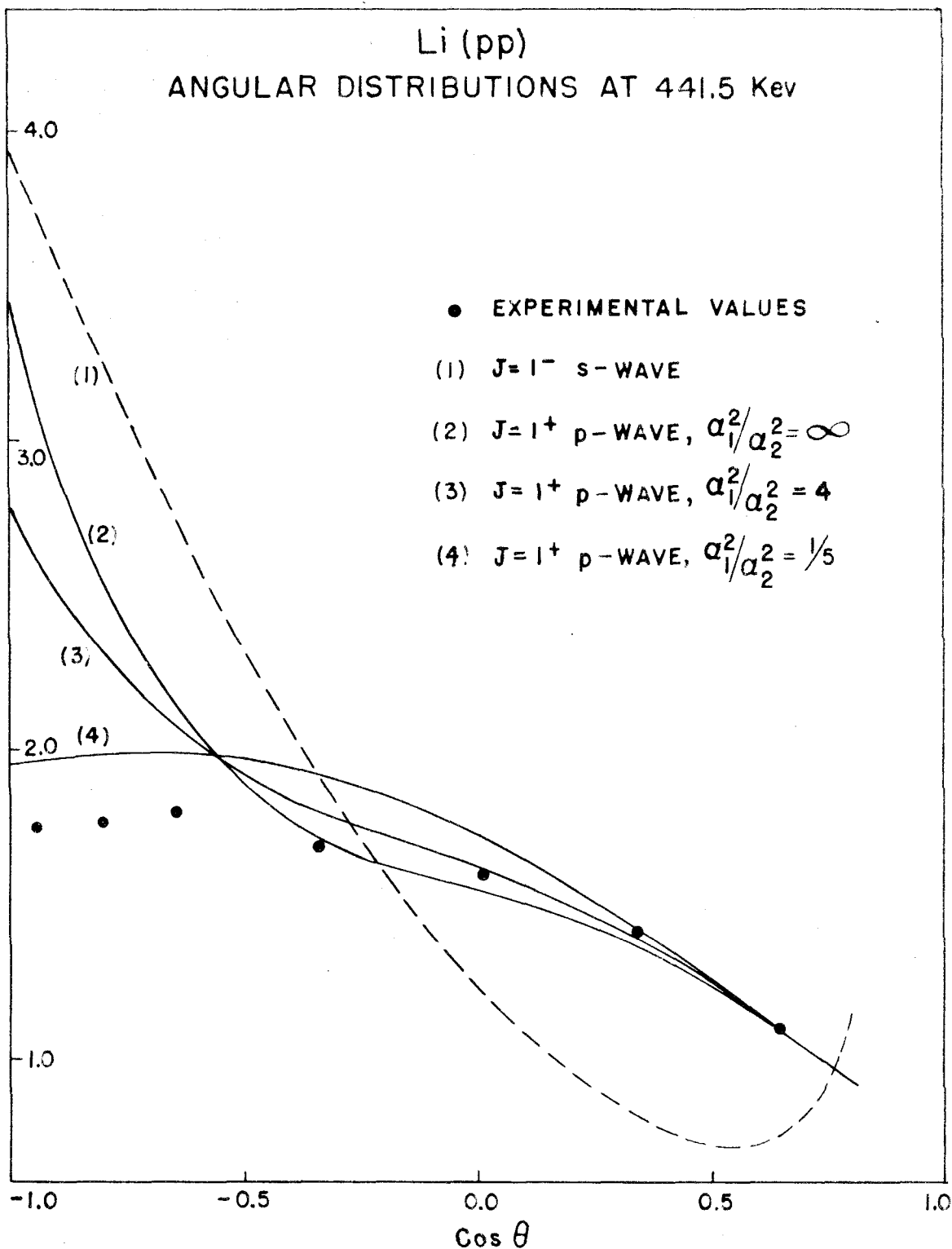


Fig. 2

The relatively good agreement of the p-wave formula with the experimental values shows that the assignment suggested by Cohen should be re-examined. The more extensive and more accurate elastic scattering data of Warters<sup>(8)</sup> and also the (p $\delta$ ) angular distributions discussed above are now available. The latter demand that the channel spin ratio  $\alpha_1^2/\alpha_2^2 = 1/5$  be used rather than Cohen's value of  $\alpha_1^2/\alpha_2^2 = 4$ . This change in channel spin ratio affects the gamma ray angular distributions greatly but has a smaller affect on the elastic scattering angular distributions as will be evident below when the formula for the latter is written down. Warters' new data also indicate that the channel spin ratio more like the value  $\alpha_1^2/\alpha_2^2 = 1/5$  used here actually fits the elastic scattering data better than the value used by Cohen. This is illustrated in Fig. 2 where the p-wave angular distributions are plotted for three channel spin ratios.

The arguments presented so far favouring p-waves over s-waves in the formation of the 440 kev resonance should be fairly convincing. One additional item can be cited which in itself probably means little, but which, when taken with all the other evidence, supports the decision in favour of p-waves. This lies in the comparison of the single particle resonance widths computed for s-, p-, and d-waves and the experimentally determined width of around 12 kev. The single particle widths are roughly

$$\Gamma_s \simeq 2kRv_0 \frac{\lambda^2}{MR^2} \simeq 750 \text{ kev,}$$

$$\Gamma_p \simeq 2kRv_1 \frac{\lambda^2}{MR^2} \simeq 100 \text{ kev,}$$

$$\Gamma_d \simeq 2kR v_2 \frac{\hbar^2}{MR^2} \simeq 3 \text{ kev.}$$

( $v_l = (F_l^2 + G_l^2)^{-1}$  is the well known Coulomb penetration factor.)

The observed width is rather small for an s-wave width and probably too large for d-waves. If one believes that the independent particle model describes  $\text{Li}^7$  and  $\text{Be}^8$  in the relevant states, then one expects that an s- or d-wave resonance would have the single particle width (within a factor of two or three), while a p-wave resonance would very likely have a rather smaller width as it would be more difficult to fit an extra proton into an already partially filled p-shell of  $\text{Li}^7$ . This argument is made by Lane<sup>(9)</sup> who presents many examples where particle widths are of about the size one would predict. This point of view is adopted in a later section of this thesis where estimates are made of the particle and radiation widths for the 17.63 and 18.14 Mev states in  $\text{Be}^8$ .

#### B. 18.14 Mev Energy Level

The experimental evidence bearing on the 18.14 Mev state in  $\text{Be}^8$  will now be discussed. As in the case of the 17.63 Mev state elastic scattering data and gamma ray cross sections are available. In addition the inelastic scattering of protons has been studied since the energy for this process is above the threshold in the region of the 18.14 Mev State.

### B.1. Gamma Radiation

The capture gamma rays associated with the 1030 kev resonance do not yield the unambiguous results that were found at the 440 kev resonance. Still there is a fair indication that again the resonant state is formed by p-waves and, except for interference effects, the resonant radiation is isotropic.

The data of Kraus<sup>(10)</sup> on the angular distribution of the hard gamma rays from this reaction are most conveniently presented by plotting as a function of energy the coefficients  $W_0$ ,  $W_1$ , and  $W_2$  which occur in the formula,

$$W(\theta) = W_0 + W_1 \cos \theta + W_2 \cos^2 \theta,$$

for the intensity of the gamma rays. These coefficients are presented in Fig. 3. The first thing to note is that  $W_2$ , the coefficient of  $\cos^2 \theta$ , does not show an anomalous behavior as do  $W_0$  and  $W_1$ . This means that the resonance, which manifests itself in the coefficients of the constant and  $\cos \theta$  terms, is either due to s-waves or p-waves with the same channel spin ratio as the 440 kev resonance. (Waves with  $l = 2$  or greater may be ruled out because of the large width of this state.)

The non-resonant  $\cos^2 \theta$  term is probably due to states excited by p-waves. s-waves of course will not give a  $\cos^2 \theta$  term and d-waves have to work against a high centrifugal barrier. These non-resonant p-waves will also account for part of the constant term and part of the  $\cos \theta$  term — the latter by interference with s-waves. The non-resonant contribution to  $W_1$  must be large enough so that when it is subtracted off, the purely resonant term

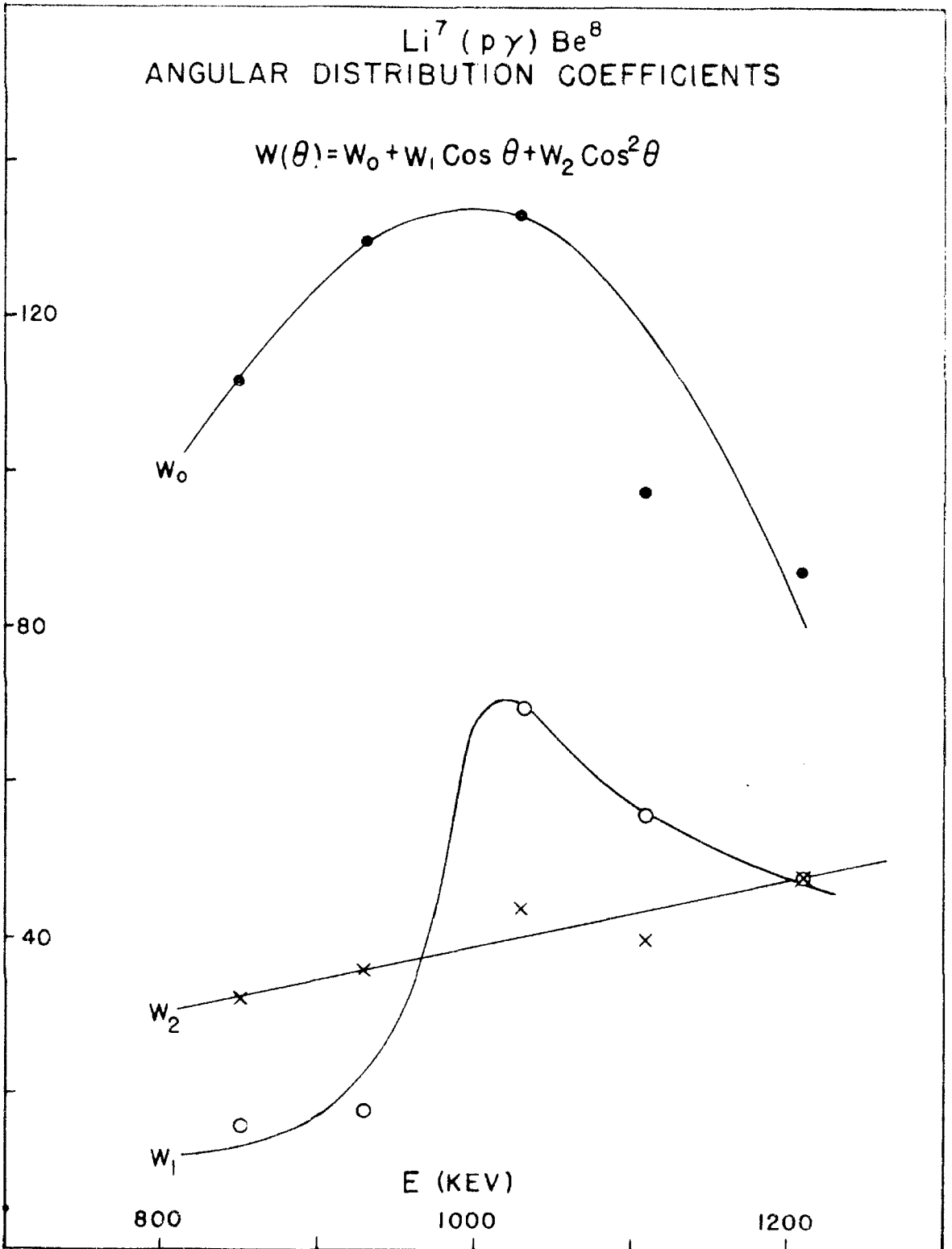


Fig. 3

remaining will have — in order of increasing energy — a negative minimum, a zero, and a positive maximum.

The resonant contribution to  $W_1$  will be due to interference between s- and p-waves, one of which will have a phase shift which is small and approximately constant (the non-resonant wave) while the other phase shift will vary from 0 to  $\pi$  radians through the resonance. The factor containing the phase shifts will be

$$\sin \delta_0 \sin \delta_1 \cos(\delta_1 + \sigma_1 - \delta_0 - \sigma_0)$$

where  $\sigma_0$  and  $\sigma_1$  are the Coulomb phase shifts for  $l = 0$  and  $l = 1$ .

( Elsewhere in this thesis  $\phi_l = \sigma_l - \sigma_0$  is used in formulas.)

If the resonance is formed by s-waves, the rapidly varying part of this term is (approximately) the factor

$$\sin \delta_0 \cos(\delta_0 + \sigma_0 - \sigma_1),$$

and in the case of a p-wave resonance it is

$$\sin \delta_1 \cos(\delta_1 + \sigma_1 - \sigma_0).$$

Now the zero in this interference term mentioned above occurs when the argument of the cosine is  $90^\circ$ . At energies in the vicinity of 1030 kev  $\sigma_1 - \sigma_0 \simeq 25^\circ$  so that the above two formulas yield values for the phase shifts when this zero occurs of

$$\delta_0 \simeq 115^\circ \text{ and } \delta_1 \simeq 65^\circ.$$

This means that the zero must occur at an energy greater than 1030 kev if the resonance is formed by s-waves and at an energy below 1030 kev if formed by p-waves. The amount in either case for a resonance the width of this one (200 kev) will be about 40 kev.

When allowance is made for the non-resonant contribution to  $W_1$ , it is fairly evident that the choice of p-waves is indicated.

In the case of the 440 kev resonance it was possible to argue



that the resonance could not have been made by s-waves, because the observed gamma width would be abnormally small for an electric dipole transition, and the interfering p-waves would have had to be abnormally large. Such arguments cannot be applied here. Although the radiation width is even less than at the 440 kev resonance, the argument against an electric dipole transition cannot be made here as this is a  $T = 0$  state (as evidenced by the lack of a companion state in  $\text{Li}^8$ ), and the final states in  $\text{Be}^8$  are also. This means that electric dipole radiation is forbidden by the electric dipole isotopic spin selection rule to the extent that  $T = 1$  and  $T = 2$  impurities are absent from the wave function. The net result would be to much reduce the electric dipole width. Also it is not possible to argue against a sizeable p-wave interference term when the  $\cos^2\theta$  term indicates that p-waves -- probably associated with a resonance of higher energy -- do appear with appreciable amplitude.

## B.2. Elastic Scattering

From the experimental cross sections for elastic scattering of protons on  $\text{Li}^7$  at the 1030 kev resonance one quantum number, the angular momentum of the compound nucleus, is fairly easily determined. This is because the interference between Coulomb and nuclear scattering is not large at angles near  $90^\circ$ , so the cross section may be represented approximately by

$$\sigma(\theta)/\sigma_c(\theta) = 1 + \frac{(1 - \cos\theta)^2}{\eta^2} \frac{2J + 1}{(2i + 1)(2I + 1)} \sin^2\delta$$

$$\approx 1 + \frac{2J + 1}{8\eta^2}$$

at  $\theta = 90^\circ$  and  $\sin \delta = 1$  (the peak of the resonance). The observed value is 2.2 while the formula gives

J	$\sigma/\sigma_c$
0	1.57
1	2.72
2	3.86

where  $\eta = \frac{Z_1 Z_2 e^2}{\hbar v} = .467$  at 1030 kev. It is evident that  $J = 2$  gives so large a value that it is improbable that the complete formula with interference terms and the contributions of non-resonant states can bring the figure down enough.

The choice then is between  $J = 0$  and  $J = 1$ . If  $J$  were 0 and the parity even, the reaction  $\text{Li}^7(p\alpha)\text{He}^4$  should show a strong resonance, but no trace of this is seen at the energies of interest. If the parity were odd, then a state of  $J = 0$  could only be formed by d-waves, and this would require a smaller particle width by a factor of two or three than that actually observed. This leaves only the possibilities  $J = 1^-$  and  $J = 1^+$  with the first formed principally by s-waves and the second by p-waves.

A decision between  $J = 1^-$  and  $J = 1^+$  requires a more or less detailed study of the possibilities that each of them offer. This is because the difference between them is only in the interference terms and these are small. (We will in this discussion assume the same channel spin ratio used previously for the 440 kev resonance. This means the angular dependence of the term containing  $\sin^2 \delta$  will

be the same for s- and p-waves. Considering the channel spin ratio as a free parameter would make fitting the data easier but would contradict the evidence of the gamma rays which are essentially isotropic.)

First of all it may be stated that a fairly good fit to the experimental data may be obtained, assuming the resonance is formed by p-waves and adding in reasonable amounts of the two s-wave phase shifts. The phase shift analysis based on this assumption will be presented later. The hard part is in convincing one's self that a similar program cannot be carried through when the central assumption is that the  $J = 1^-$  s-wave phase shift is resonant.

The formula which we will try to fit to the experimental data is

$$\begin{aligned} \sigma(\theta) / \sigma_c(\theta) = & 1 + \frac{3}{8\eta^2} (1 - \mu)^2 \sin^2 \delta \\ & - \frac{3}{4\eta} \mu(1 - \mu) \sin \delta \cos(\delta + 2\phi_1 - \xi) \\ & + \frac{(1 - \mu)^2}{8\eta^2} (3\sin^2 \beta_1 + 5\sin^2 \beta_2) \\ & - \frac{(1 - \mu)}{4\eta} \left[ 3\sin \beta_1 \cos(\beta_1 - \xi) + 5\sin \beta_2 \cos(\beta_2 - \xi) \right] \\ & + \frac{3}{4\eta^2} \mu(1 - \mu)^2 \sin \delta \left[ \frac{1}{6} \sin \beta_1 \cos(\beta_1 - \delta - 2\phi_1) + \frac{5}{6} \sin \beta_2 \cos(\beta_2 - \delta - 2\phi_1) \right] \end{aligned}$$

where  $\mu = \cos \theta$ ,  $\sigma_c(\theta) = \eta^2 / (1 - \mu)^2$  is the Coulomb cross section,  $\xi = -\eta \log \frac{1 - \mu}{2}$ ,  $\delta$  is the p-wave phase shift,  $\beta_1$  the  $J = 1^-$  s-wave shift, and  $\beta_2$  the  $J = 2^-$  s-wave phase shift. When we wish to consider  $\beta_1$  as the resonant phase shift, it is not

necessary to assume the p-waves have  $J = 1$  as has been done in this formula. Choosing other values of  $J$  will have its major effect in modifying the constants  $-3/8$ ,  $3/4$ , etc.—which appear in terms relating to the p-wave phase shift and not in significantly changing the character of the various terms.

In Fig. 4 and Fig. 5 are plotted the angular distribution at 900 kev for the s- and p-wave phase shift formulas along with the experimental data. It is apparent that in neither case is a very good fit obtained, nor does there seem to be any reason for choosing one or the other of the two possibilities. But, for the one of the two choices which is the correct one, it should be possible to improve the fit considerably by adding terms to the formula with small phase shifts corresponding to additional states which are not resonant at this energy.

If  $\beta_1$  is the resonant phase shift, it seems likely that  $\beta_2$  will be the largest among the non-resonant phase shifts. The contribution of  $\beta_2$  can be obtained by using the curves in Fig. 4 by subtracting one and multiplying by  $5/3$ . Focusing our attention on  $\theta = 90^\circ$  ( $\mu = 0$ ), we see that the observed cross section is larger than the value obtained for any  $\sin \beta_1$  between 0.2 and 0.7. Thus a positive correction is needed, but a reasonably small positive  $\beta_2$  gives a contribution with the wrong sign. A small negative  $\beta_2$  will give a correction of the correct sign but is not compatible with the observed angular distributions at lower energies. This is because at energies below 700 or 800 kev the resonant phase shift will be small while  $\beta_2$ , which has no resonance in this region, could not be very different from its value at 900 kev. Therefore  $\beta_2$  would give

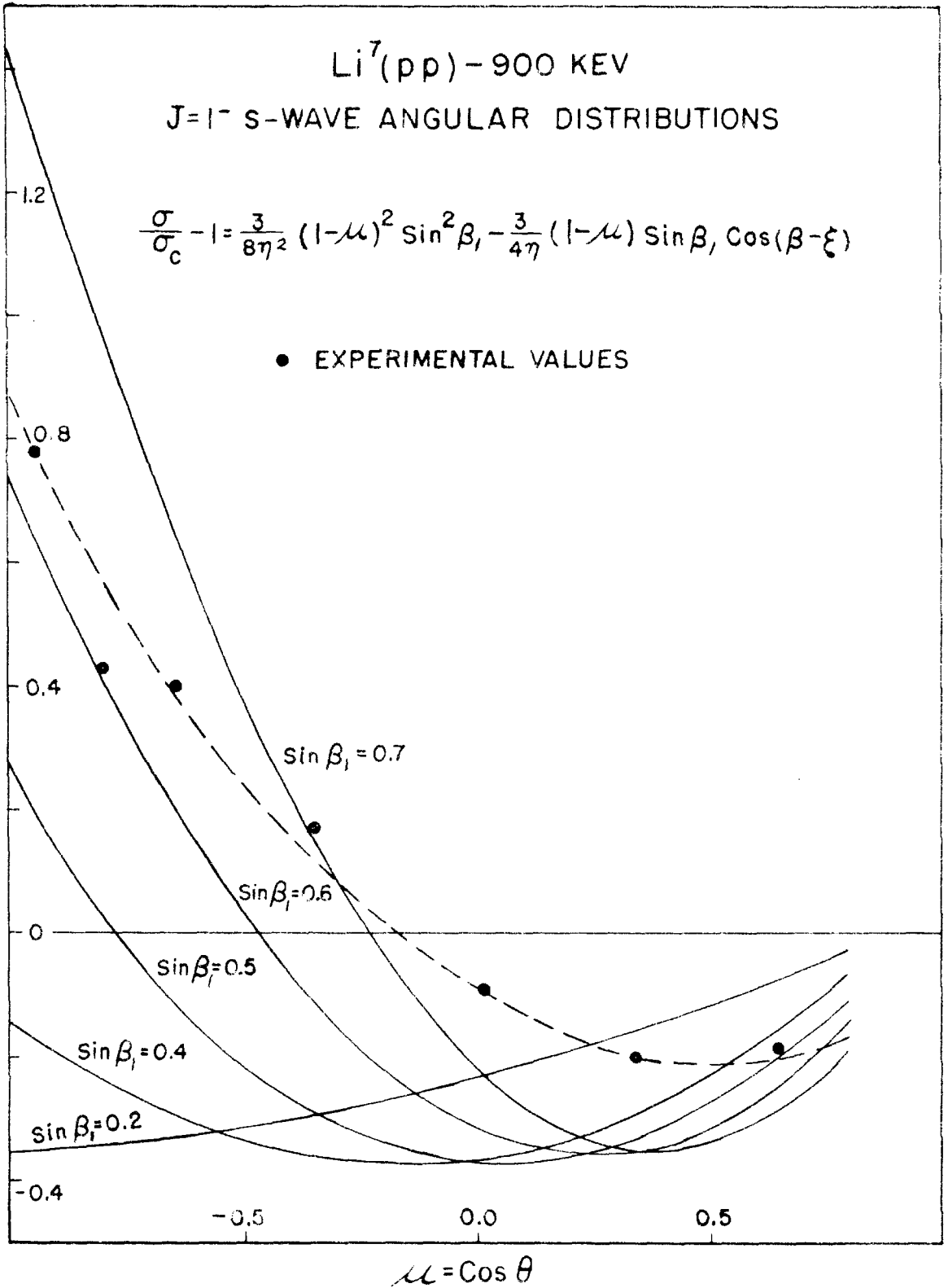


Fig.4

much the same positive contribution to  $\sigma/\sigma_c$  that it is designed to give at 900 kev, and, lacking a sizeable contribution from  $\beta_1$ , we would get  $\sigma/\sigma_c > 1$  at all measured angles and especially at the backward angles. The contrary is observed in the experimental data which shows that  $\sigma/\sigma_c < 1$  except at the smallest angle measured ( $50^\circ$ ).

If, instead of using  $\beta_2$  in trying to improve the fit with the assumption that  $\beta_1$  is resonant, one tries using a p-wave phase shift for this purpose, it is seen that such improvement is possible. From Fig. 3 we see that a p-wave will give a positive contribution at all angles. If  $\sin\beta_1$  is chosen small enough - say  $\sin\beta_1 \approx 0.2$  - and  $\sin\delta$  large enough - about 0.4 will do - then a rough fit is obtained. This pretty much forces us to the view, which further attempts at fitting the data in this energy region confirm, that the p-wave phase shift is the resonant one.

The argument just presented may be summarized by saying that an s-wave resonance should show a larger dip in the cross section before the peak of the resonance than is actually observed.

In Fig. 7 the data taken at  $E_p = 1030$  kev is plotted along with the simple s- and p-wave angular distributions using the phase shift  $\pi/2$  as this is the peak of the resonance. Here again a first glance will indicate no preference for either the s- or the p-wave. If the s-wave is believed to be resonant, it is necessary to use additional terms in the phase shift formula which will give a negative contribution at backward angles. A p-wave will do this only if its phase shift is large, i.e.  $\delta + 2\phi_1 > \pi/2$ . This presumes a p-wave resonance at lower energies, and the region there is well

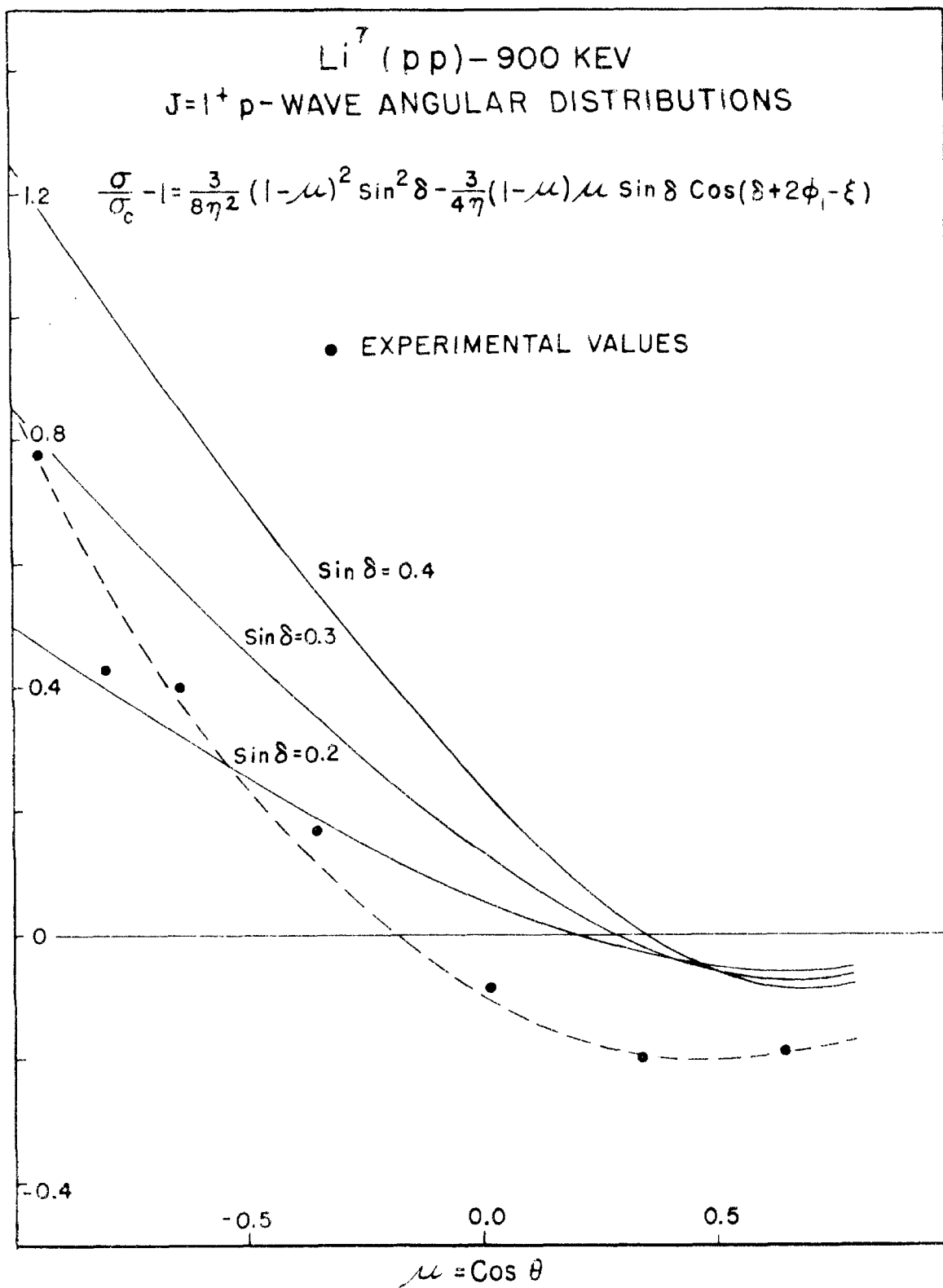


Fig. 5

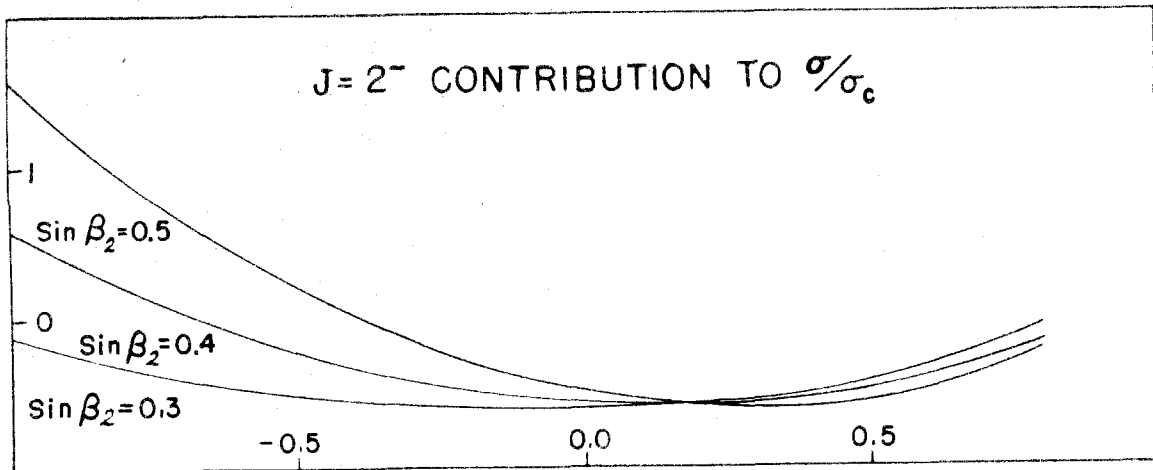


Fig. 6

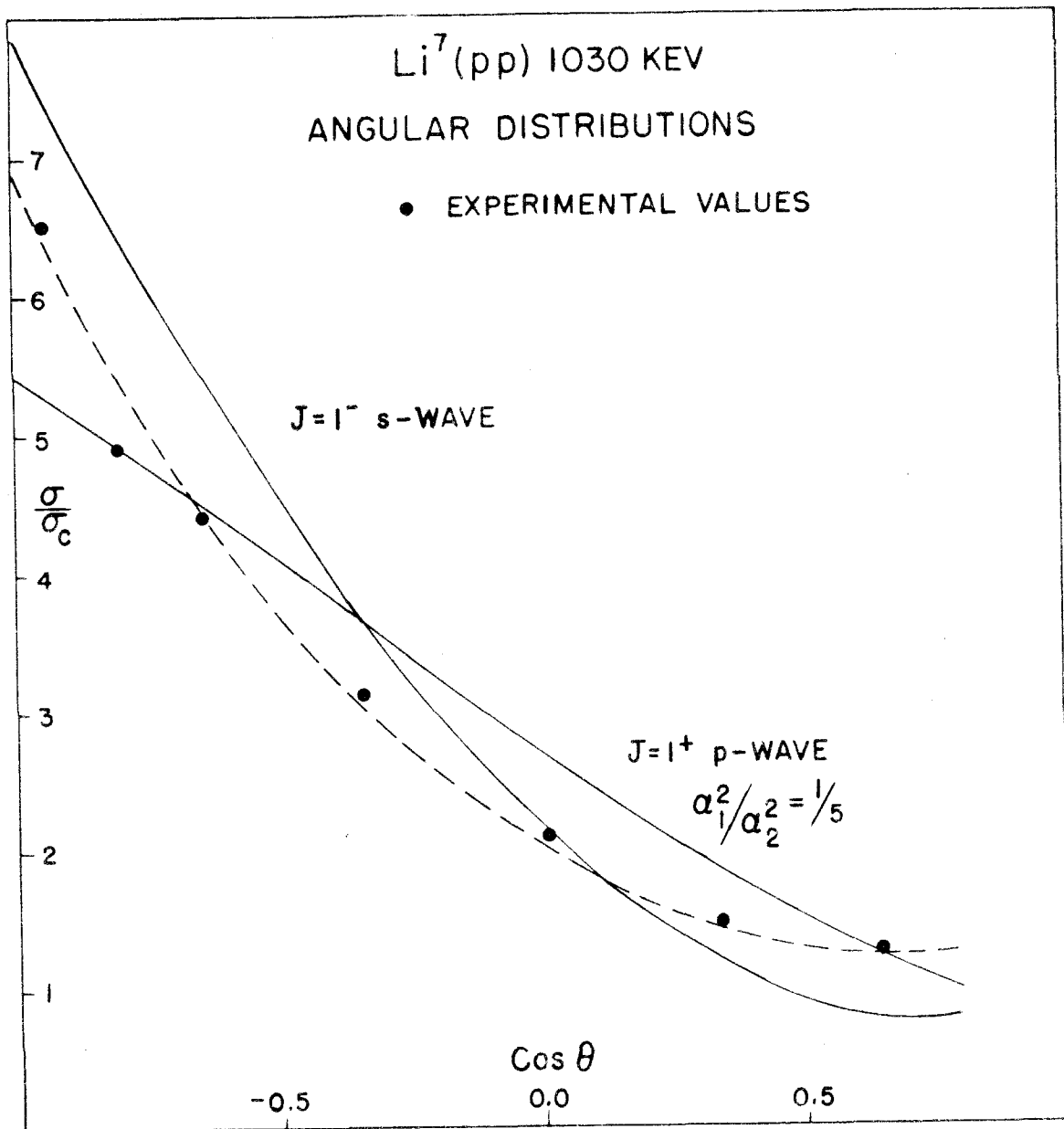


Fig. 7



enough explored so that this possibility can be ruled out. (There is of course the 440 kev resonance, but it is too narrow to have any effect this far from its peak.) The  $J = 2^-$  s-wave can also give a negative contribution at angles near  $180^\circ$ , but at best only half as large as is needed. Also, it will give a negative contribution at forward angles which makes the agreement with experiment there poorer.

The contrary assumption - that the resonance is formed by p-waves - gives an angular distribution which is easily corrected by an s-wave of moderate size. A glance at Fig. 6 shows that with  $\sin\beta_2 \simeq 0.5$  there is a positive contribution at backward angles and a negative contribution near  $90^\circ$  and at forward angles which is just what is needed to correct the p-wave angular distribution.

Since the two arguments presented here based on the elastic scattering data - one in the energy region below the peak of the resonance and the other at the peak - are by no means a sure proof that the resonance is formed by p-waves, it would be helpful if it could be similarly shown that in the region above the resonance peak the evidence also favours p-waves. This however, does not appear to be easy, for the s-wave contribution in this region is large. This is consistent with the picture we are arguing for, namely that the resonance is formed by p-waves, but in addition there is an increasing  $J = 2^-$  phase shift associated with a broad s-wave level having its peak around 2 Mev.

### B.3. Inelastic Scattering

The inelastic scattering of protons on  $\text{Li}^7$  has been measured by Mozer, Fowler, and Lauritsen<sup>(11)</sup> at 1050, 1140, 1240 kev and many different angles. The differential cross section at 1050 kev is  $\sigma(\theta) = 3.3 - .35 \cos \theta$  millibarns/steradian indicating states of different parities contributing. Most likely these are formed by s- and p-waves, but from the inelastic scattering data alone it is not possible to tell whether the resonant state is due to s- or p-waves. If the state is formed by p-waves and has  $J = 1$  the angular distribution will be

$$1 + \frac{(5\alpha_1^2 - \alpha_2^2)(\beta_1^2 - 2\beta_0^2)}{10} P_2(\cos \theta)$$

where  $\beta_0$  and  $\beta_1$  are the channel spin coefficients for the emitted proton and  $\text{Li}^7$  in its first excited state. The  $P_2(\cos \theta)$  term will vanish if we use the channel spin ratio  $\alpha_1^2/\alpha_2^2 = 1/5$  that was proposed on the basis of gamma ray angular distribution.

The inelastic scattering width may easily be estimated if we take  $J = 1$  for the compound nucleus and  $\Gamma \approx 200$  kev. Then at the peak of the resonance

$$\sigma(\theta) = \frac{3}{8k^2} \frac{\Gamma_p \Gamma_{p'}}{\Gamma^2}$$

which yields  $\Gamma_{p'} \approx 9$  kev when the value 3.3 millibarns quoted above is used. This may be compared with the single particle widths computed for s- and p-waves which are

$$\Gamma_s \approx 1100 \text{ kev,}$$

$$\Gamma_p \approx 130 \text{ kev.}$$

The observed inelastic scattering width is rather small when compared with either of these.

### C. Phase Shift Analysis

In the preceding sections it was decided that the 17.63 and 18.14 Mev states in  $\text{Be}^8$  have  $J = 1^+$ , channel spin ratio  $\alpha_1^2/\alpha_2^2 = 1/5$ , and are formed by p-wave protons in the bombardment of  $\text{Li}^7$ . It is plausible to assume that the main non-resonant contributions to the scattering are due to s-waves which leads us to the following phase shift formula for the elastic scattering :

$$\begin{aligned} \frac{\sigma(\theta)}{\sigma_c(\theta)} = & 1 + \frac{3}{8\eta^2} \frac{\Gamma_p}{\Gamma} \sin^2 \delta \left[ 1 + \frac{(5\alpha_1^2 - \alpha_2^2)^2}{50} P_2(\mu) \right] (1-\mu)^2 \\ & - \frac{3}{4\eta} \sqrt{\frac{\Gamma_p}{\Gamma}} \sin \delta \cos(\delta + 2\phi_1 - \xi) \mu(1-\mu) + \frac{1}{8\eta^2} \left[ 3 \sin^2 \beta_1 + 5 \sin^2 \beta_2 \right] (1-\mu)^2 \\ & - \frac{1}{4\eta} \left[ 3 \sin \beta_1 \cos(\beta_1 - \xi) + 5 \sin \beta_2 \cos(\beta_2 - \xi) \right] (1-\mu) \\ & + \frac{3}{4\eta^2} \sqrt{\frac{\Gamma_p}{\Gamma}} \sin \delta \left[ \alpha_1^2 \sin \beta_1 \cos(\beta_1 - \delta - 2\phi_1) + \alpha_2^2 \sin \beta_2 \cos(\beta_2 - \delta - 2\phi_1) \right] (1-\mu)^2 \end{aligned}$$

where  $\mu = \cos \theta$ ,  $\sigma_c(\theta) = \eta^2/(1-\mu)^2$  is the Coulomb cross section,  $\xi = -\eta \log(1-\mu)/2$ ,  $\delta$  is the p-wave phase shift,  $\beta_1$  and  $\beta_2$  are the s-wave phase shifts, and  $\phi_1$  is the Coulomb phase shift.  $\alpha_1^2$  and  $\alpha_2^2$  are taken to be 1/6 and 5/6 respectively.

In this formula the quantities relating to the Coulomb scattering are known from theory. Since no comparable theory of nuclei exists, the specifically nuclear quantities -  $\delta$ ,  $\beta_1$ ,  $\beta_2$ , and  $\Gamma_p/\Gamma$  - must be regarded as arbitrary parameters to be adjusted to fit the experimental cross sections.

Some restrictions can be placed on these parameters, and these should be observed. Thus, in the vicinity of a resonance the phase shift should have the form

$$e^{2i\delta} - 1 = \frac{-i\Gamma/2}{E - E_0 + i\Gamma/2}$$

or, equivalently,

$$\frac{E - E_0}{\Gamma/2} = -\cot \delta$$

Also, the energy dependence of  $\Gamma$  should be largely controlled by the penetration factor so that it can be written as  $\Gamma = 2s\gamma^2$  with  $\gamma^2$  (the "reduced width") constant. Then

$$-s \cot \delta = \frac{E - E_0}{\gamma^2},$$

when plotted against  $E$ , should be a straight line in the vicinity of the resonance.

The procedure used in fitting the cross section curves was this : at a dozen or more energies a variety of sets of phase shifts were tried until a fairly good fit to the observed angular distribution was obtained. Then  $-s_1 \cot \delta$  was plotted as a function of energy, and a smooth curve was drawn through the points which took the form of a straight line in the neighbourhood of either resonance. The slope of this curve at the resonant energies gave the reduced widths of the two levels. It was found by this method that  $\beta_2$  was increasing rapidly with energy, so it was also assumed to have a resonance (but at a higher energy than Warters' measurements go), and  $-s_0 \cot \beta_2$  was treated in the same manner as  $-s_1 \sin \delta$ .

The other s-wave phase shift -  $\beta_1$  - was found to be small, so it was assumed to be essentially constant over the entire energy range. In the lower half of the energy range, where  $\beta_2$  is still fairly small, this assumption is warranted by the observed angular distributions, but at higher energies the effects of  $\beta_2$  would cover up any but a large increase in the size of  $\beta_1$ . Finally,

$$\frac{\Gamma_p}{\Gamma} = \frac{\Gamma_p}{\Gamma_p + \Gamma_{p'}}$$

was computed by finding the reduced widths for both elastic and inelastic scattering at 1030 kev and giving to both  $\Gamma_p$  and  $\Gamma_{p'}$  the energy dependence of their penetration factors. The 440 kev resonance is below the threshold for inelastic scattering, so  $\Gamma_{p'}/\Gamma = 1$  in that energy range.

The fit obtained to the experimental data is on the whole pretty good. It could have been better, had more effort been expended or had machine computation been available. At energies above the 1030 kev resonance the fit becomes rather poor. Probably the reason is that the effects of higher energy p-wave resonances are beginning to be felt. This supposition is supported by the fact that there is a constantly increasing  $\cos^2 \theta$  term in the gamma ray cross section in this region.

The experimental data and the calculated cross section curves are compared in Figs. 8 - 14. The phase shifts  $\delta$  and  $\beta_2$  used are presented in Figs. 15 - 18 in the form  $-s_1 \cot \delta$  and  $-s_0 \cot \beta_2$ .

$\beta_1$  was taken to be .03 for energies less than 700 kev and .04 above that.

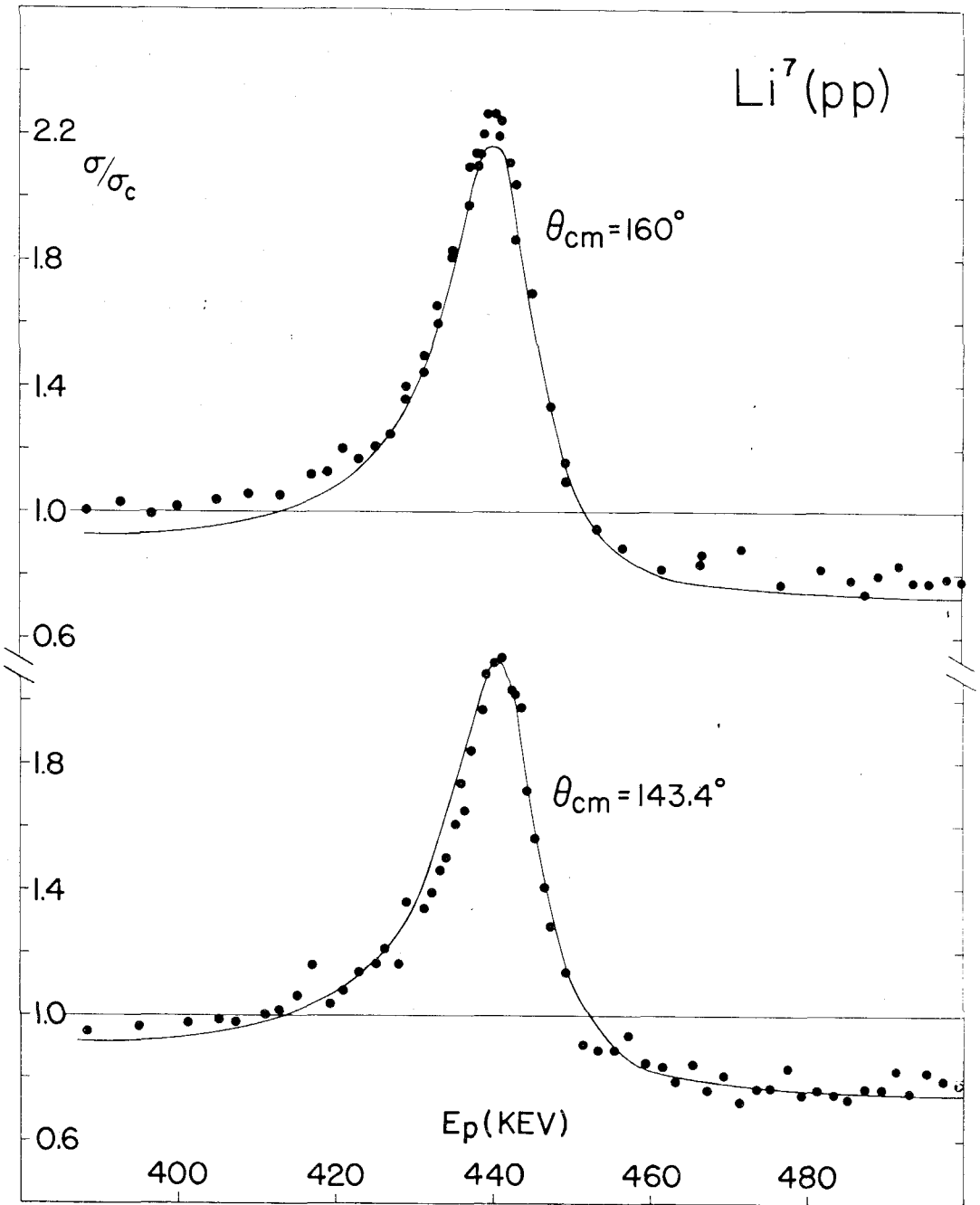


Fig. 8

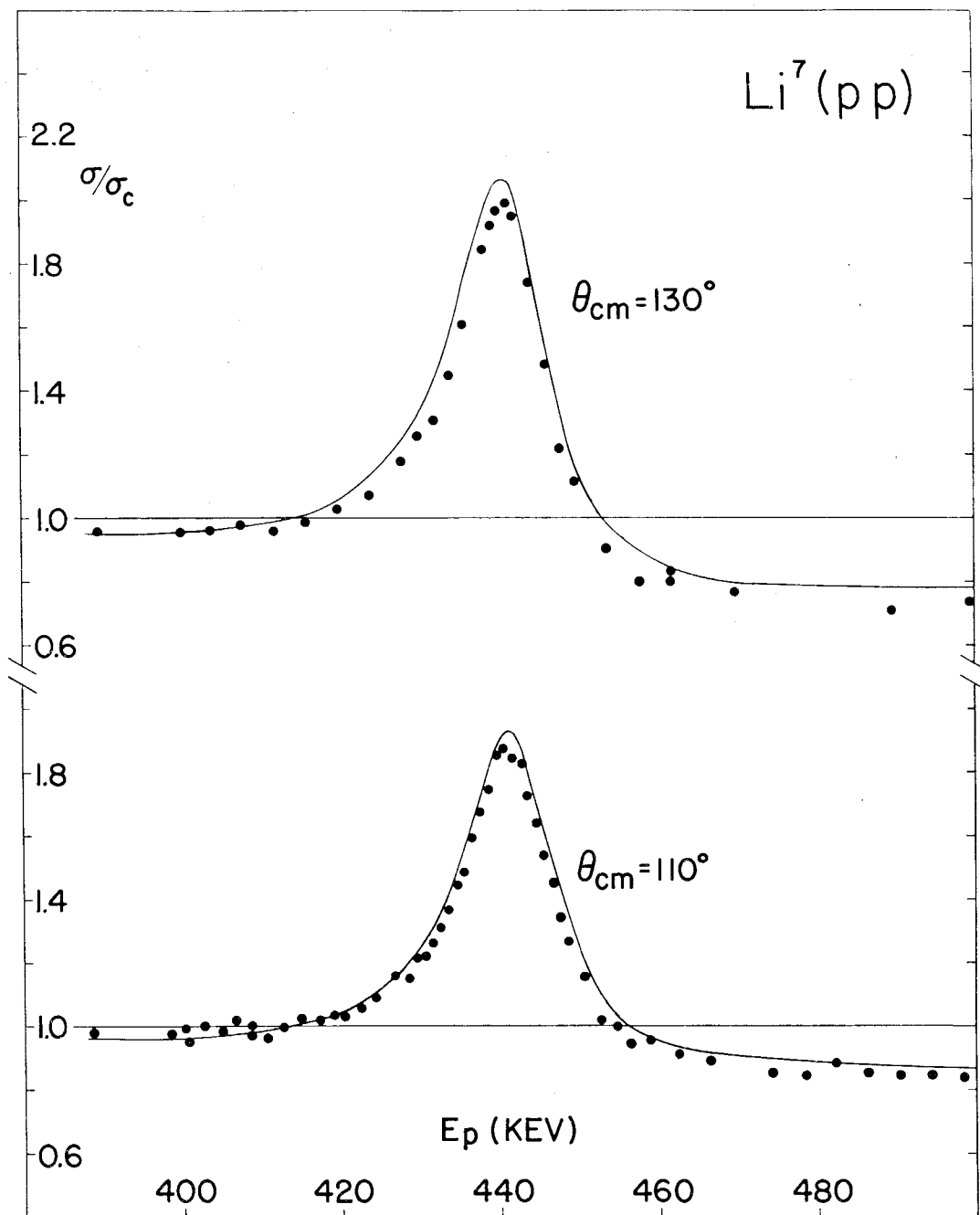


Fig.9

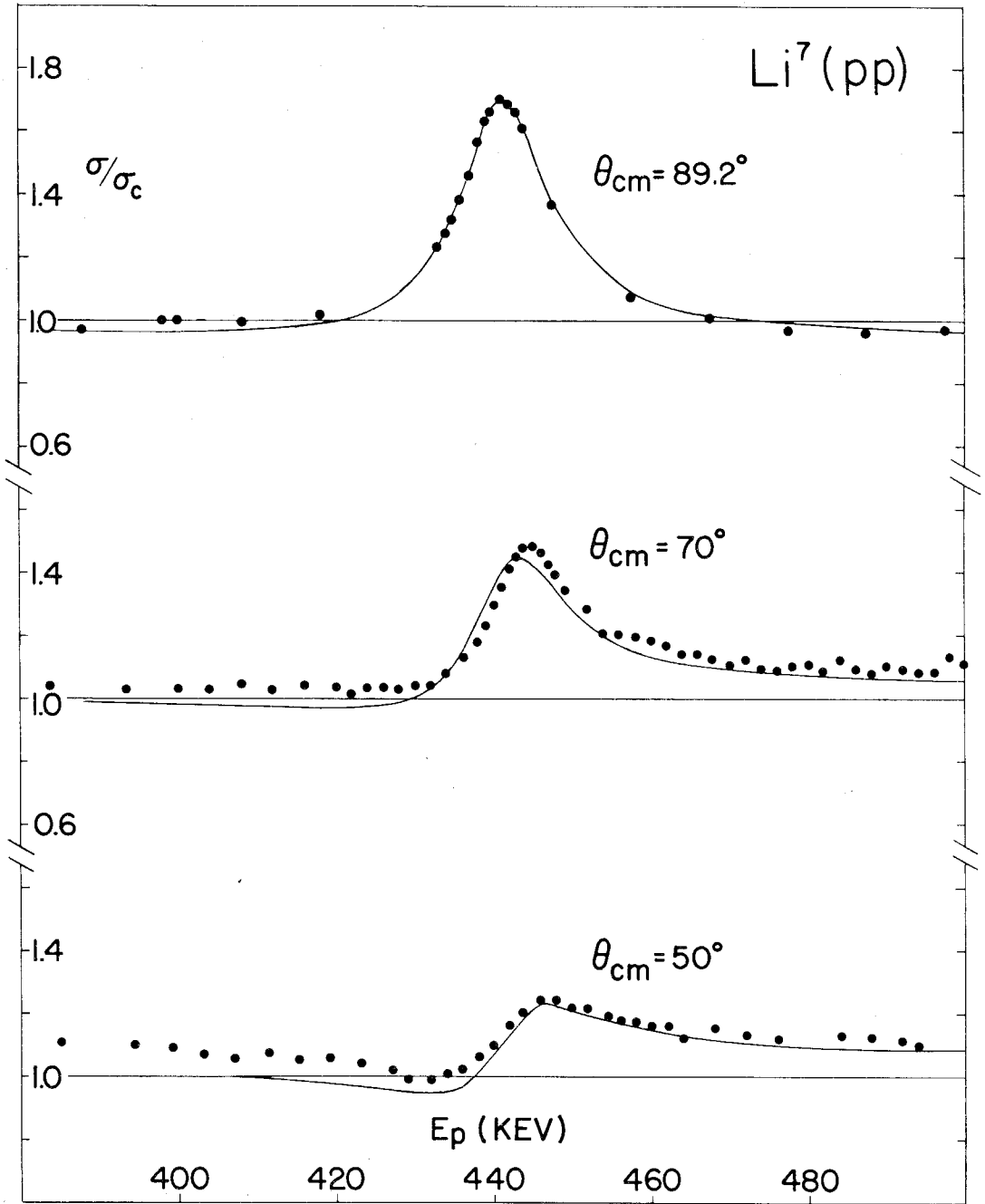


Fig. 10



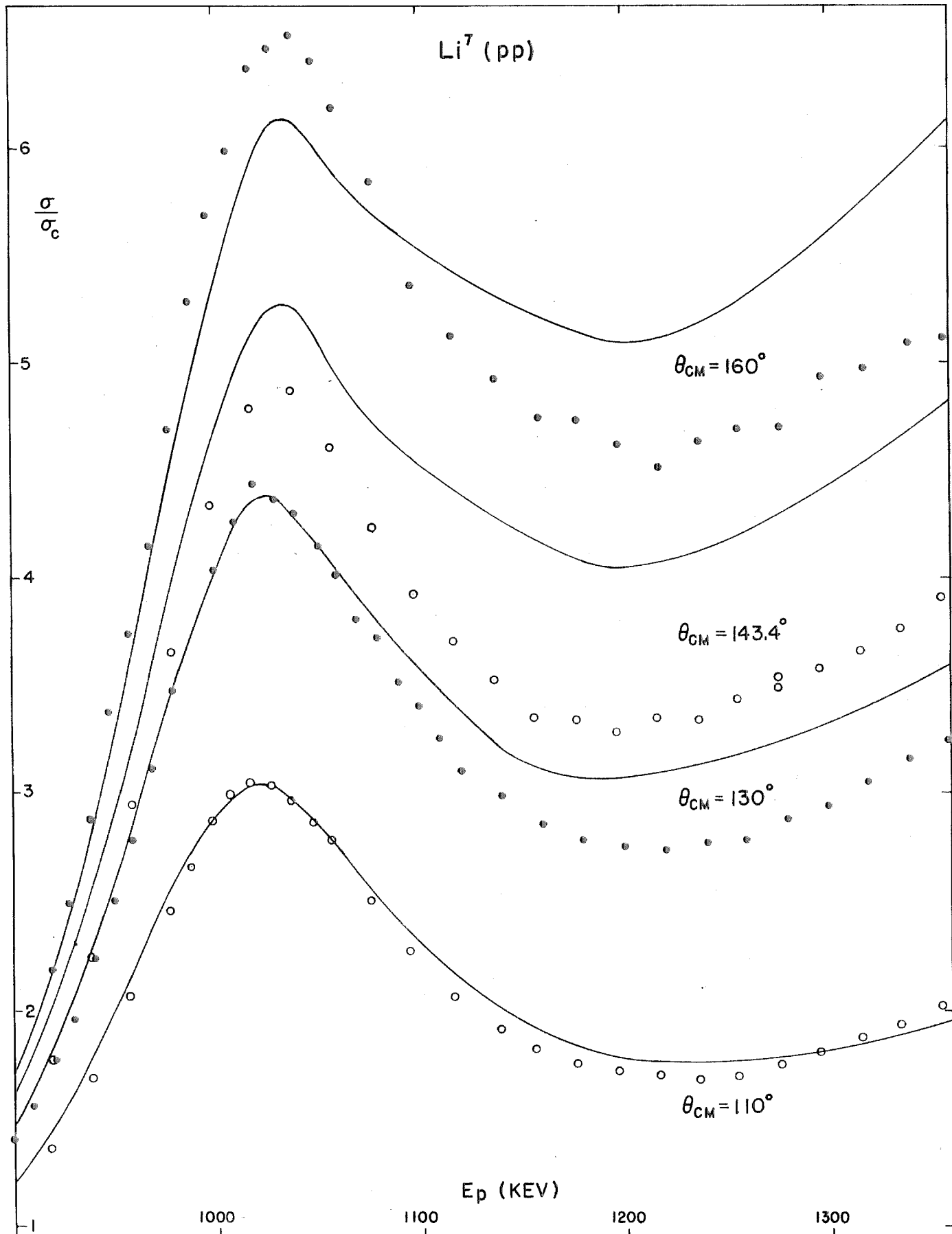


Fig. 11

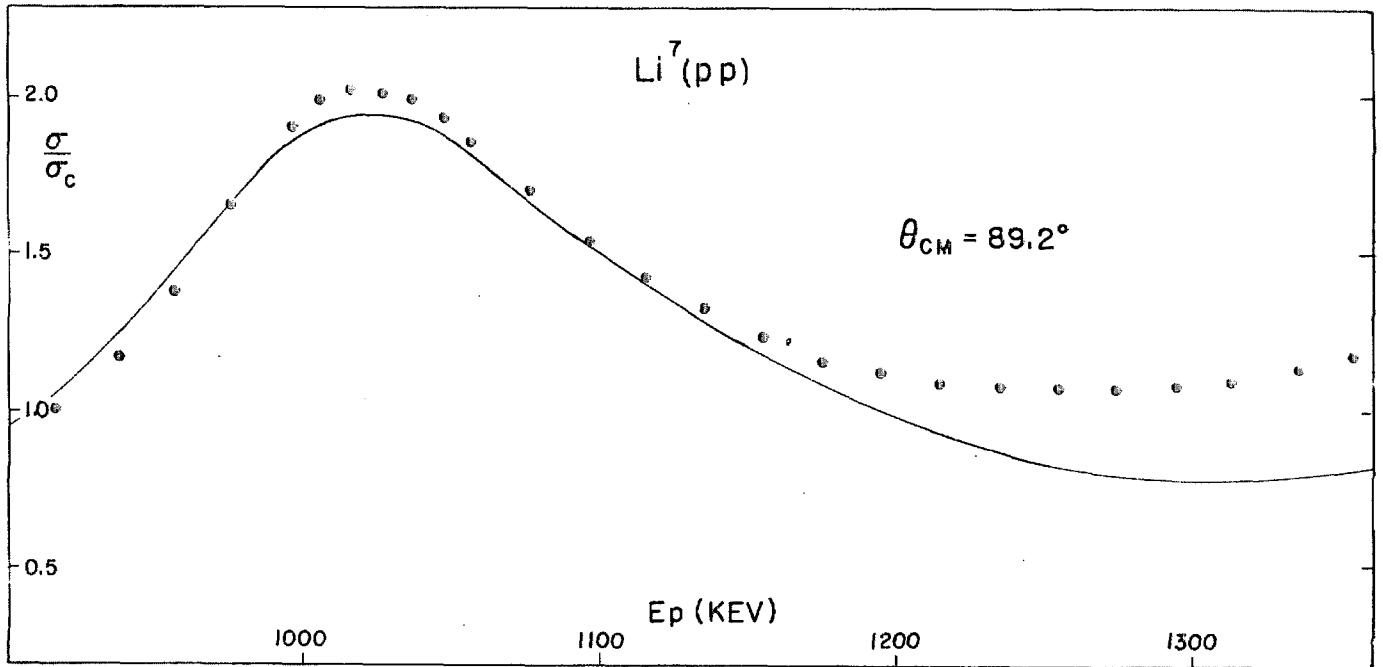


Fig. 12

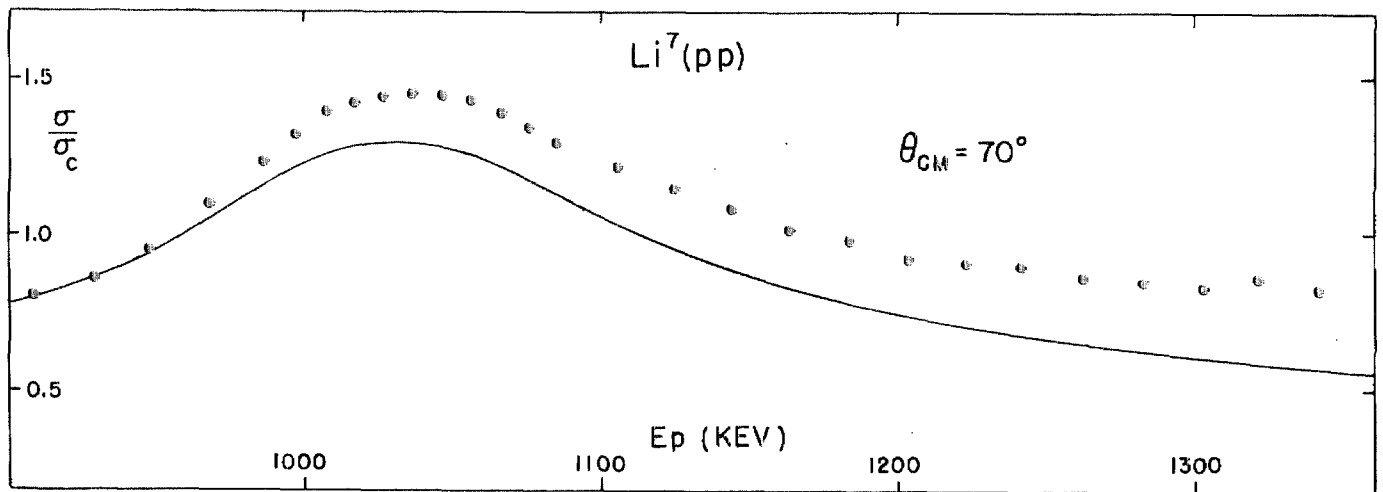


Fig. 13

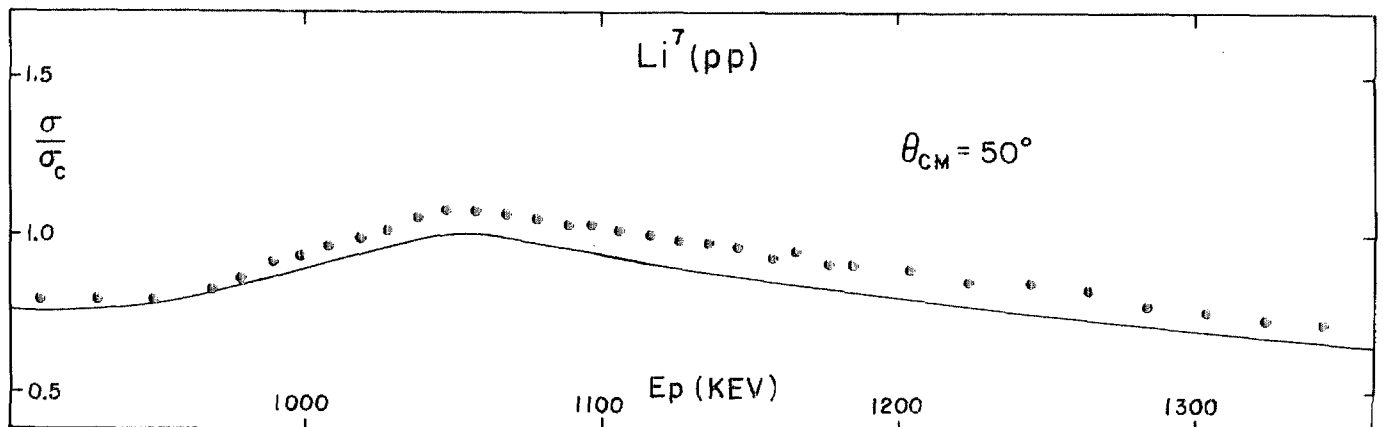


Fig. 14

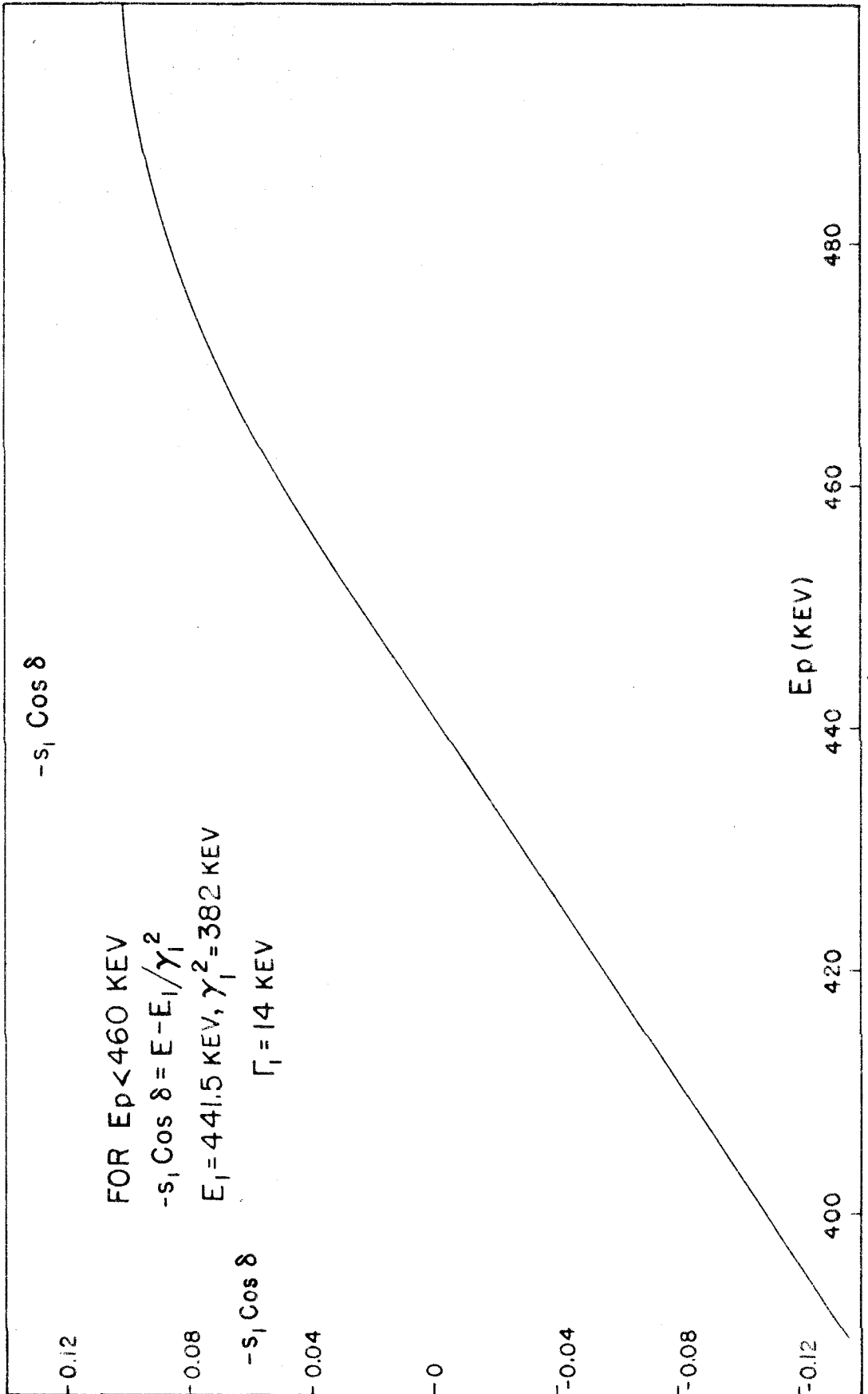


Fig. 15

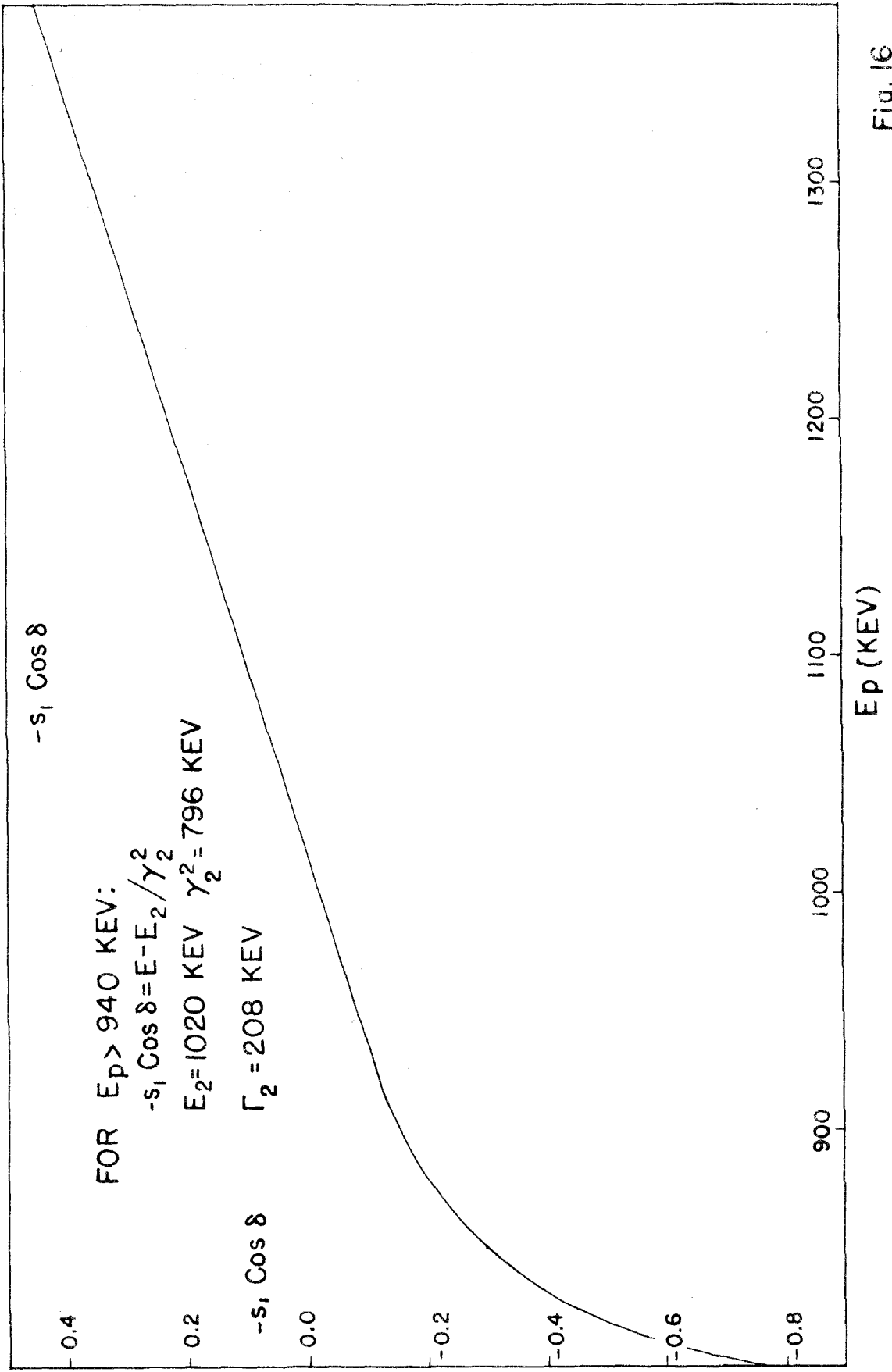


Fig. 16

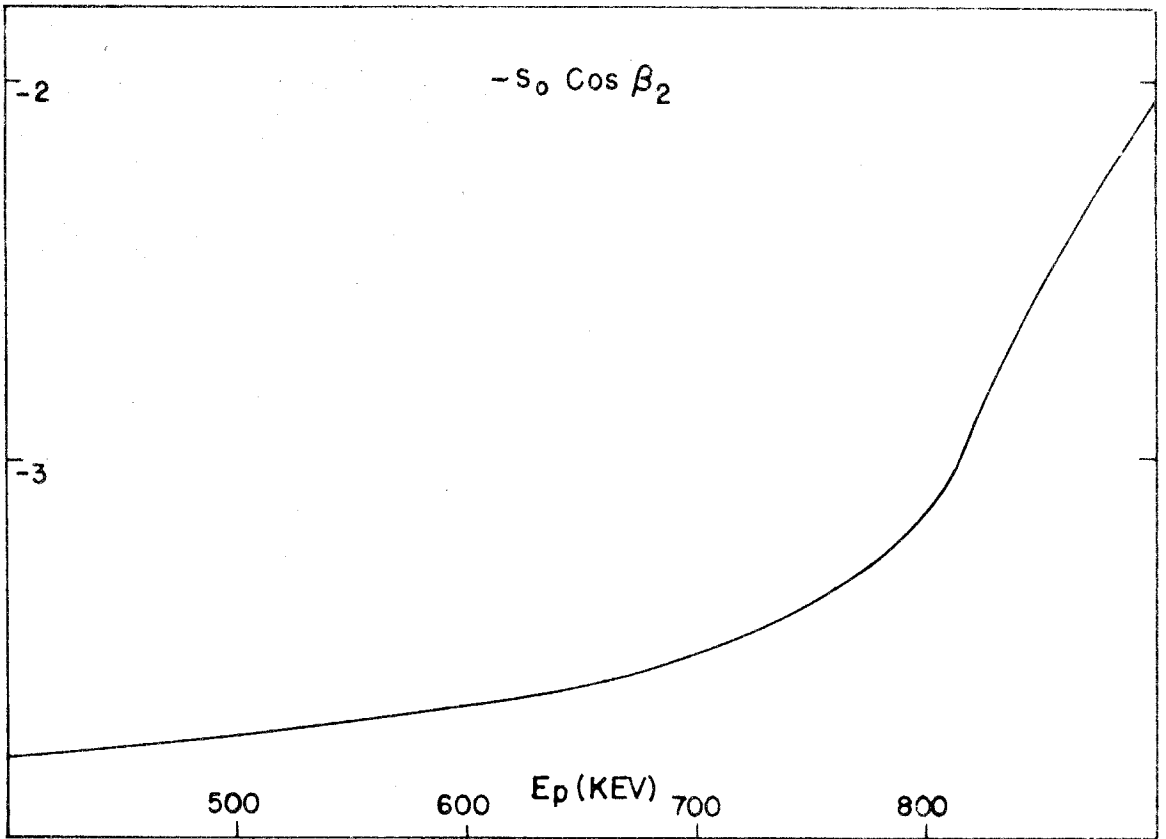


Fig. 17

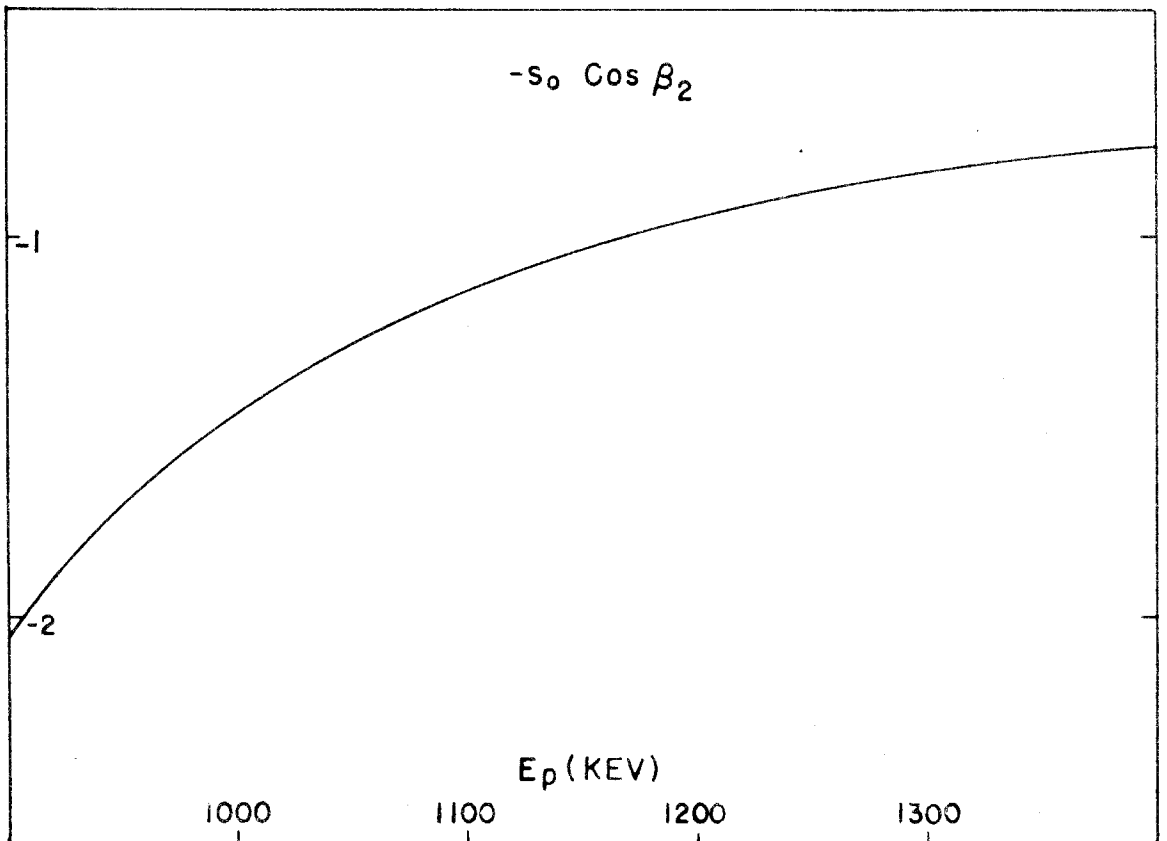


Fig. 18

### III. INDEPENDENT PARTICLE MODEL WAVE FUNCTIONS AND LEVEL PARAMETERS

The numerous successes of the shell model proposed by Haxel, Jensen, and Suess<sup>(12)</sup> and Mayer<sup>(13)</sup> in accounting for many of the properties of the ground states of nuclei have renewed interest in the independent particle picture of nuclei. Despite the serious theoretical objections to such a conception of the structure of nuclei, there has been sufficient experimental verification of some of the predictions of one or another such model of nuclei to encourage attempts at correlating experimental data through the use of independent wave functions.

In the following sections independent particle wave functions will be developed for the various nuclei involved in the reactions being considered here. This will be done for the LS (Russell-Saunders) and *jj* coupling models. On the basis of these wave functions predictions regarding observable features of the reactions are made and then compared with the actual observations.

Since the manifold of wave functions which can be constructed for seven or eight particles is very large, a number of "plausible assumptions" will be made in order to reduce the field that must be surveyed to manageable proportions.

The first such assumption is that  $\text{Li}^7$  and  $\text{Be}^8$  in all the states of interest have filled 1s shells and the remaining particles in the 1p shell. In the case of *jj* coupling the 1p shell is broken down into two sub-shells - the  $1p_{3/2}$  and the  $1p_{1/2}$  - with the latter being higher in energy in keeping with the rules postulated for

the  $jj$  coupling model by Mayer and Jensen. Another such assumption is that in the LS case the low states will have the maximum possible degree of spatial symmetry. This will be true if the major part of the nuclear force is of the Wigner or Majorana type.

Further assumptions will be made when they are needed to resolve ambiguities which may arise in choosing this or that wave function to describe a nuclear state.

#### A. Wave Functions for $jj$ Coupling Model

In this coupling scheme we start from single particle wave functions having a definite angular momentum,  $j$ , and compound them into wave functions of given  $J$  (total angular momentum for the whole nucleus), parity, isotopic spin, and configuration. The configuration is the number of particles in each sub-shell.

The nuclei being considered here ( $\text{Li}^7$  and  $\text{Be}^8$ ) have four particles in a filled  $1s_{1/2}$  shell which can be neglected in writing down the wave functions. The remaining three or four particles will be in the  $1p_{3/2}$  and  $1p_{1/2}$  shells, and we will thus concern ourselves mainly with constructing three and four particle wave functions describing the unfilled shells.

The single particle wave functions used to describe a particle in the  $1p_{3/2}$  and  $1p_{1/2}$  shells are listed in Table I. The notation used in the table is fairly standard: the  $Y_l^m(\Omega)$  are normalized spherical harmonics,  $\alpha$  and  $\beta$  are spin functions,  $U_{1p}(r)$  is the radial wave function characteristic of the  $1p$  shell, and the various square roots appearing are vector addition

(Clebsch - Gordan) coefficients. When it is desirable to specify a certain particle - say number three - we write  $\phi_{3/2}^{3/2}(3)$ ,  $Y_1^0(3)$ ,  $\alpha(3)$  etc.

A few words about the radial wave functions are necessary. If they are used to describe bound particles (the two neutrons in the 1p shell are always in this category in the cases of interest here), they may be regarded as, say, the characteristic functions for a square well with the usual exponentially decaying behavior at large distances. On the other hand if they are to describe particles which are unbound they should be the usual Coulomb wave functions at large distances, and in the interior region of the nucleus should satisfy the interior region eigenvalue problem specified by Wigner and Eisenbud<sup>(14)</sup> in their theory of resonance reactions. The actual form of the interior region solutions will be sufficiently similar in both cases for us to neglect the difference between them. In the following the radial wave functions will be suppressed in writing down wave functions (or equivalently considered as part of the  $Y_l^m(\Omega)$ ) except when their values are actually needed.

The next step is the construction of wave functions for two identical particles (two neutrons or two protons). These wave functions must of course be antisymmetric as is required by the Pauli principle. If the two particles are in the  $1p_{3/2}$  shell, the wave function will be symmetric if the total angular momentum is 3 or 1 and antisymmetric if 2 or 0. If they are both in the  $1p_{1/2}$  shell, an angular momentum of 1 corresponds to a symmetric wave function and 0 to the antisymmetric one. In the case that one of the identical particles is in the  $1p_{3/2}$  shell and the other in the  $1p_{1/2}$



shell, angular momenta of 2 and 1 are obtained. But the wave functions obtained using the vector addition coefficients have no special symmetry and for our purposes, therefore, need explicit antisymmetrization. These two particle functions are listed in Table 2. The particle numbers 1 and 2 are used to designate neutrons. The same functions are used with particle numbers 3 and 4 for protons.

Table 1

$1p_{3/2}$  and  $1p_{1/2}$  single particle wave functions,  $\phi_j^m$

$$\phi_{3/2}^{3/2} = U_{1p}(r) Y_1^1(\Omega) \alpha$$

$$\phi_{3/2}^{1/2} = U_{1p}(r) \left[ \sqrt{\frac{1}{3}} Y_1^1(\Omega) \beta + \sqrt{\frac{2}{3}} Y_1^0(\Omega) \alpha \right]$$

$$\phi_{3/2}^{-1/2} = U_{1p}(r) \left[ \sqrt{\frac{2}{3}} Y_1^0(\Omega) \beta + \sqrt{\frac{1}{3}} Y_1^{-1}(\Omega) \alpha \right]$$

$$\phi_{3/2}^{-3/2} = U_{1p}(r) Y_1^{-1}(\Omega) \beta$$

$$\phi_{1/2}^{1/2} = U_{1p}(r) \left[ \sqrt{\frac{2}{3}} Y_1^1(\Omega) \beta - \sqrt{\frac{1}{3}} Y_1^0(\Omega) \alpha \right]$$

$$\phi_{1/2}^{-1/2} = U_{1p}(r) \left[ \sqrt{\frac{1}{3}} Y_1^0(\Omega) \beta - \sqrt{\frac{2}{3}} Y_1^{-1}(\Omega) \alpha \right]$$

Table 2

Two particle wave functions

$$(1p_{3/2})^2$$

$$\phi_2^2(12) = \sqrt{\frac{1}{2}} \phi_{3/2}^{3/2}(1) \phi_{3/2}^{1/2}(2) - \sqrt{\frac{1}{2}} \phi_{3/2}^{1/2}(1) \phi_{3/2}^{3/2}(2)$$

$$\phi_2^1(12) = \sqrt{\frac{1}{2}} \phi_{3/2}^{3/2}(1) \phi_{3/2}^{-1/2}(2) - \sqrt{\frac{1}{2}} \phi_{3/2}^{-1/2}(1) \phi_{3/2}^{3/2}(2)$$

$$\phi_2^0(12) = \sqrt{\frac{1}{4}} \phi_{3/2}^{3/2}(1) \phi_{3/2}^{-3/2}(2) + \sqrt{\frac{1}{4}} \phi_{3/2}^{1/2}(1) \phi_{3/2}^{-1/2}(2) - \sqrt{\frac{1}{4}} \phi_{3/2}^{-1/2}(1) \phi_{3/2}^{1/2}(2) - \sqrt{\frac{1}{4}} \phi_{3/2}^{-3/2}(1) \phi_{3/2}^{3/2}(2)$$

$$\phi_2^{-1}(12) = \sqrt{\frac{1}{2}} \phi_{3/2}^{1/2}(1) \phi_{3/2}^{-3/2}(2) - \sqrt{\frac{1}{2}} \phi_{3/2}^{-3/2}(1) \phi_{3/2}^{1/2}(2)$$

$$\phi_2^{-2}(12) = \sqrt{\frac{1}{2}} \phi_{3/2}^{-1/2}(1) \phi_{3/2}^{-3/2}(2) - \sqrt{\frac{1}{2}} \phi_{3/2}^{-3/2}(1) \phi_{3/2}^{-1/2}(2)$$

$$\phi_0^0(12) = \sqrt{\frac{1}{4}} \phi_{3/2}^{3/2}(1) \phi_{3/2}^{-3/2}(2) - \sqrt{\frac{1}{4}} \phi_{3/2}^{1/2}(1) \phi_{3/2}^{-1/2}(2) + \sqrt{\frac{1}{4}} \phi_{3/2}^{-1/2}(1) \phi_{3/2}^{1/2}(2) - \sqrt{\frac{1}{4}} \phi_{3/2}^{-3/2}(1) \phi_{3/2}^{3/2}(2)$$

$$(1p_{3/2})(1p_{1/2})$$

$$\psi_2^2(12) = \sqrt{\frac{1}{2}} \phi_{3/2}^{3/2}(1) \phi_{1/2}^{1/2}(2) - \sqrt{\frac{1}{2}} \phi_{1/2}^{1/2}(1) \phi_{3/2}^{3/2}(2)$$

$$\psi_2^1(12) = \sqrt{\frac{1}{8}} \phi_{3/2}^{3/2}(1) \phi_{1/2}^{-1/2}(2) + \sqrt{\frac{3}{8}} \phi_{3/2}^{1/2}(1) \phi_{1/2}^{1/2}(2) - \sqrt{\frac{1}{8}} \phi_{1/2}^{-1/2}(1) \phi_{3/2}^{3/2}(2) - \sqrt{\frac{3}{8}} \phi_{1/2}^{1/2}(1) \phi_{3/2}^{1/2}(2)$$

$$\psi_2^0(12) = \sqrt{\frac{1}{4}} \phi_{3/2}^{1/2}(1) \phi_{1/2}^{-1/2}(2) + \sqrt{\frac{1}{4}} \phi_{3/2}^{-1/2}(1) \phi_{1/2}^{1/2}(2) - \sqrt{\frac{1}{4}} \phi_{1/2}^{-1/2}(1) \phi_{3/2}^{1/2}(2) - \sqrt{\frac{1}{4}} \phi_{1/2}^{1/2}(1) \phi_{3/2}^{-1/2}(2)$$

$$\psi_2^{-1}(12) = \sqrt{\frac{3}{8}} \phi_{3/2}^{-1/2}(1) \phi_{1/2}^{-1/2}(2) + \sqrt{\frac{1}{8}} \phi_{3/2}^{-3/2}(1) \phi_{1/2}^{1/2}(2) - \sqrt{\frac{3}{8}} \phi_{1/2}^{-1/2}(1) \phi_{3/2}^{-1/2}(2) - \sqrt{\frac{1}{8}} \phi_{1/2}^{-1/2}(1) \phi_{3/2}^{-3/2}(2)$$

$$\psi_2^{-2}(12) = \sqrt{\frac{1}{2}} \phi_{3/2}^{-3/2}(1) \phi_{1/2}^{-1/2}(2) - \sqrt{\frac{1}{2}} \phi_{1/2}^{-1/2}(1) \phi_{3/2}^{-3/2}(2)$$

Table 2 (continued)

$$\psi_1^1(12) = \sqrt{\frac{3}{8}} \phi_{3/2}^{3/2}(1) \phi_{1/2}^{-1/2}(2) - \sqrt{\frac{1}{8}} \phi_{3/2}^{1/2}(1) \phi_{1/2}^{1/2}(2) - \sqrt{\frac{3}{8}} \phi_{1/2}^{5/2}(1) \phi_{3/2}^{3/2}(2) + \sqrt{\frac{1}{8}} \phi_{1/2}^{1/2}(1) \phi_{3/2}^{5/2}(2)$$

$$\psi_1^0(12) = \sqrt{\frac{1}{4}} \phi_{3/2}^{1/2}(1) \phi_{1/2}^{-1/2}(2) - \sqrt{\frac{1}{4}} \phi_{3/2}^{-1/2}(1) \phi_{1/2}^{1/2}(2) - \sqrt{\frac{1}{4}} \phi_{1/2}^{-1/2}(1) \phi_{3/2}^{1/2}(2) + \sqrt{\frac{1}{4}} \phi_{1/2}^{1/2}(1) \phi_{3/2}^{-1/2}(2)$$

$$\psi_1^{-1}(12) = \sqrt{\frac{1}{8}} \phi_{3/2}^{-1/2}(1) \phi_{1/2}^{-1/2}(2) - \sqrt{\frac{3}{8}} \phi_{3/2}^{-3/2}(1) \phi_{1/2}^{1/2}(2) - \sqrt{\frac{1}{8}} \phi_{1/2}^{-1/2}(1) \phi_{3/2}^{-1/2}(2) + \sqrt{\frac{3}{8}} \phi_{1/2}^{1/2}(1) \phi_{3/2}^{-3/2}(2)$$

$$(1p_{1/2})^2$$

$$\psi_0^0(12) = \sqrt{\frac{1}{2}} \phi_{1/2}^{1/2}(1) \phi_{1/2}^{-1/2}(2) - \sqrt{\frac{1}{2}} \phi_{1/2}^{-1/2}(1) \phi_{1/2}^{1/2}(2)$$

#### A.1. $J = 3/2^-$ Wave Functions for $\text{Li}^7$

According to the Mayer - Jensen shell model, the  $\text{Li}^7$  ground state should belong to the configuration  $(1p_{3/2})^3$  with the two neutrons paired to give zero spin, and the only proton in the  $1p_{3/2}$  shell giving rise of necessity to the correct spin of  $3/2$ . The wave function describing this situation is not, however, an eigenfunction of the total isotopic spin as it should be, and it is necessary to consider in addition the possibility of the two neutrons adding to give spin 2. Two wave functions corresponding to  $J_n = 0$  and  $J_n = 2$  can therefore be constructed. These are given in Table 3.

The curly brackets over the particle numbers 1 and 2 indicate that the function is antisymmetric in the interchange of those particles. On occasion a bar will be used to indicate symmetry, but, also, these indications of the symmetry properties of the function may be omitted when they are unimportant for the matters of hand.

Table 3

Li<sup>7</sup> ground state wave functions

	neutrons			proton	J
	j <sub>1</sub>	j <sub>2</sub>	J <sub>n</sub>	j <sub>3</sub> =J <sub>p</sub>	
A <sub>1</sub>	3/2	3/2	2	3/2	3/2
A <sub>2</sub>	3/2	3/2	0	3/2	3/2

$$A_1^{3/2}(\overline{123}) = \sqrt{\frac{2}{5}} \phi_2^2(n) \phi_{3/2}^{-1/2}(p) - \sqrt{\frac{2}{5}} \phi_2^1(n) \phi_{3/2}^{1/2}(p) + \sqrt{\frac{1}{5}} \phi_2^0(n) \phi_{3/2}^{3/2}(p)$$

$$A_1^{1/2}(\overline{123}) = \sqrt{\frac{2}{5}} \phi_2^2(n) \phi_{3/2}^{-3/2}(p) - \sqrt{\frac{1}{5}} \phi_2^0(n) \phi_{3/2}^{1/2}(p) + \sqrt{\frac{1}{5}} \phi_2^1(n) \phi_{3/2}^{3/2}(p)$$

$$A_1^{-1/2}(\overline{123}) = \sqrt{\frac{2}{5}} \phi_2^1(n) \phi_{3/2}^{-3/2}(p) - \sqrt{\frac{1}{5}} \phi_2^0(n) \phi_{3/2}^{-1/2}(p) + \sqrt{\frac{2}{5}} \phi_2^{-2}(n) \phi_{3/2}^{3/2}(p)$$

$$A_1^{-3/2}(\overline{123}) = \sqrt{\frac{1}{5}} \phi_2^0(n) \phi_{3/2}^{-3/2}(p) - \sqrt{\frac{2}{5}} \phi_2^{-1}(n) \phi_{3/2}^{-1/2}(p) + \sqrt{\frac{2}{5}} \phi_2^{-2}(n) \phi_{3/2}^{1/2}(p)$$

$$A_2^{3/2}(\overline{123}) = \phi_0^0(n) \phi_{3/2}^{3/2}(p)$$

$$A_2^{1/2}(\overline{123}) = \phi_0^0(n) \phi_{3/2}^{1/2}(p)$$

$$A_2^{-1/2}(\overline{123}) = \phi_0^0(n) \phi_{3/2}^{-1/2}(p)$$

$$A_2^{-3/2}(\overline{123}) = \phi_0^0(n) \phi_{3/2}^{-3/2}(p)$$

As mentioned above the wave functions  $A_1$  and  $A_2$  are not eigenfunctions of the total isotopic spin, but certain linear combinations of them will be. These we wish to find.

The total isotopic spin operator  $T^2$  is defined to operate on isotopic spin wave functions which have not been used up to now. Let us call one of the three particle wave functions  $f(\overline{123})$  and append to it the appropriate isotopic spin wave functions :  $f(\overline{123})n(1)n(2)p(3)$ .  $n$  and  $p$  are the neutron and proton isotopic spin wave functions. In keeping with the generalized Pauli principle this may now be replaced by the completely antisymmetric form:  $F(\overline{123}) = f(\overline{123})n(1)n(2)p(3) - f(\overline{321})n(3)n(2)p(1) - f(\overline{132})n(1)n(3)p(2)$   
 $= (I - P_{13} - P_{23}) f(\overline{123})n(1)n(2)p(3)$  .

$P_{13}$  and  $P_{23}$  are the permutation operators which exchange particles 1 and 3, and 2 and 3, respectively.

Now  $T^2$  is applied to  $F$ . Using

$$T^2 n(1)n(2)p(3) = \frac{7}{4} n(1)n(2)p(3) + n(3)n(2)p(1) + n(1)n(3)p(2)$$

(the result of an elementary computation with vector addition coefficients), we get

$$\begin{aligned} T^2 F(\overline{123}) &= \left[ \frac{7}{4} f(123) - f(321) - f(132) \right] n(1)n(2)p(3) \\ &\quad - \left[ \frac{7}{4} f(321) - f(132) - f(123) \right] n(3)n(2)p(1) \\ &\quad - \left[ \frac{7}{4} f(132) - f(123) - f(321) \right] n(1)n(3)p(2) \end{aligned}$$

It is now evident that  $T^2$  operating on  $F(\overline{123})$  is completely equivalent to  $\tau^2 = 7/4 I - P_{13} - P_{23}$  operating on  $f(\overline{123})$ . For our purposes it is more convenient to use the more compact  $f(\overline{123})$  and the associate operator  $\tau^2$ .

Below matrix elements of  $\tau^2$  will be calculated, and thus those of  $P_{13}$  and  $P_{23}$  will be needed. It shortens the work if it is noted now that they are equal. This can be seen by writing down a matrix element

$$(f_1(\tilde{1}\tilde{2}3) | P_{13} | f_2(\tilde{1}\tilde{2}3))$$

and then exchanging 1 for 2 in it :

$$(f_1(\tilde{2}\tilde{1}3) | P_{23} | f_2(\tilde{2}\tilde{1}3)).$$

This can be done as the particle numbers are dummy variables. Then, because of the antisymmetry of the wave functions, the matrix element is equal to

$$(f_1(\tilde{1}\tilde{2}3) | P_{23} | f_2(\tilde{1}\tilde{2}3)) ,$$

which establishes the above assertion. Also, it is to be noted that the permutation operators are scalars with respect to rotation so that  $(\alpha JM | P | \alpha' J'M') = 0$

unless  $J = J'$  and  $M = M'$ , and also the

$$(\alpha JM | P | \alpha' JM)$$

are independent of  $M$ . This means, that in computing matrix elements, we can restrict ourselves to a single projection of the angular momentum.

The required matrix elements are computed by decomposing the wave functions into the single particle wave functions and performing the required interchanges. The calculations are rather messy, so only the results will be quoted here :

$$P_{13} = \begin{pmatrix} -3/4 & 5/4 \\ 5/4 & 1/4 \end{pmatrix},$$

$$\tau^2 = \begin{pmatrix} 13/4 & -5/2 \\ -5/2 & 5/4 \end{pmatrix}.$$

The matrix of  $\tau^2$  has as eigenvalues and eigenvectors

$$\tau^2 = 3/4, \begin{pmatrix} \sqrt{1/6} \\ \sqrt{5/6} \end{pmatrix} ; \quad \tau^2 = \frac{15}{4}, \begin{pmatrix} \sqrt{5/6} \\ -\sqrt{1/6} \end{pmatrix}$$

The corresponding wave functions are

$$B_1 = \sqrt{\frac{1}{6}} A_1 + \sqrt{\frac{5}{6}} A_2 \quad T = 1/2 ,$$

$$B_2 = \sqrt{\frac{5}{6}} A_1 - \sqrt{\frac{1}{6}} A_2 \quad T = 3/2 .$$

Since it is known that the ground state of  $\text{Li}^7$  has  $J = 3/2$  and  $T = 1/2$ ,  $B_1$  must be the wave function of  $\text{Li}^7$  if the jj coupling model is correct. This state has a magnetic moment of 3.04 nuclear magnetons which is in fair agreement with the experimental value of 3.26 nuclear magnetons.

#### A.2. $J = 1/2^-$ Wave Functions for $\text{Li}^7$

The first excited state of  $\text{Li}^7$  is observed to have a spin of  $1/2$ . Since it is less than a half million volts above the ground state, it may be expected that it belongs to the same configuration -  $(1p_{3/2})^3$  - as the ground state. There is only one such function which is given in Table 4 below.

The isotopic spin of this wave function is obtained by computing the expected value of  $\tau^2$  which turns out to be  $3/4$ . Thus  $A_3$  has  $T = 1/2$  which agrees with what is observed experimentally.

Table 4

$J = 1/2^-$  wave function

	neutrons			proton	
	$j_1$	$j_2$	$J_n$	$j_3 = J_p$	$J$
$A_3$	3/2	3/2	2	3/2	1/2

$$A_3^{1/2} = \sqrt{\frac{2}{5}} \phi_2^2(12) \phi_{3/2}^{-3/2}(3) - \sqrt{\frac{3}{10}} \phi_2^1(12) \phi_{3/2}^{-1/2}(3) + \sqrt{\frac{1}{5}} \phi_2^0(12) \phi_{3/2}^{1/2}(3) - \sqrt{\frac{1}{10}} \phi_2^{-1}(12) \phi_{3/2}^{3/2}(3)$$

$$A_3^{-1/2} = \sqrt{\frac{1}{10}} \phi_2^1(12) \phi_{3/2}^{-3/2}(3) - \sqrt{\frac{1}{5}} \phi_2^0(12) \phi_{3/2}^{-1/2}(3) + \sqrt{\frac{3}{10}} \phi_2^{-1}(12) \phi_{3/2}^{1/2}(3) - \sqrt{\frac{2}{5}} \phi_2^{-2}(12) \phi_{3/2}^{3/2}(3)$$

A.3.  $J = 1^+$  Wave Functions for  $Be^8$

The analysis of the first part of this thesis indicated that both the 17.63 Mev and 18.14 Mev states in  $Be^8$  have  $J = 1^+$ . Therefore we wish to consider all wave functions having this spin and parity and formed from 1p shell single particle wave functions. There are thirteen such functions (each having 3 projections), and they are collected in Table 5. Only the  $M = 1$  projections are needed in what follows, so only they will be listed.

Table 5

$J = 1^+$  wave functions

	neutrons			protons			$J$	configuration
	$j_1$	$j_2$	$J_n$	$j_3$	$j_4$	$J_p$		
$C_1$	3/2	3/2	2	3/2	3/2	2	1	$(1p_{3/2})^4$



Table 5 (continued)

	neutrons			protons			J	configuration
	$j_1$	$j_2$	$J_n$	$j_3$	$j_4$	$J_p$		
$c_2$	3/2	3/2	2	3/2	1/2	2	1	} $(1p_{3/2})^3(1p_{1/2})$
$c_3$	3/2	1/2	2	3/2	3/2	2	1	
$c_4$	3/2	3/2	2	3/2	1/2	1	1	
$c_5$	3/2	1/2	1	3/2	3/2	2	1	
$c_6$	3/2	3/2	0	3/2	1/2	1	1	
$c_7$	3/2	1/2	1	3/2	3/2	0	1	
$c_8$	3/2	1/2	2	3/2	1/2	2	1	
$c_9$	3/2	1/2	2	3/2	1/2	1	1	
$c_{10}$	3/2	1/2	1	3/2	1/2	2	1	
$c_{11}$	3/2	1/2	1	3/2	1/2	1	1	
$c_{12}$	3/2	1/2	1	1/2	1/2	0	1	} $(1p_{3/2})(1p)$
$c_{13}$	1/2	1/2	0	3/2	1/2	1	1	

$$c_1 = \sqrt{\frac{2}{10}} \phi_2^2(n) \phi_2^{-1}(p) - \sqrt{\frac{3}{10}} \phi_2^1(n) \phi_2^0(p) + \sqrt{\frac{3}{10}} \phi_2^0(n) \phi_2^1(p) - \sqrt{\frac{2}{10}} \phi_2^{-1}(n) \phi_2^2(p)$$

Table 5 (continued)

$$c_2 = \sqrt{\frac{2}{10}} \phi_2^2(n) \psi_2^{-1}(p) - \sqrt{\frac{3}{10}} \phi_2'(n) \psi_2^0(p) + \sqrt{\frac{3}{10}} \phi_2^0(n) \psi_2'(p) - \sqrt{\frac{2}{10}} \phi_2^{-1}(n) \psi_2^2(p)$$

$$c_3 = -\sqrt{\frac{2}{10}} \psi_2^2(n) \phi_2^{-1}(p) + \sqrt{\frac{3}{10}} \psi_2'(n) \phi_2^0(p) - \sqrt{\frac{3}{10}} \psi_2^0(n) \phi_2'(p) + \sqrt{\frac{2}{10}} \psi_2^{-1}(n) \phi_2^2(p)$$

$$c_4 = \sqrt{\frac{3}{5}} \phi_2^2(n) \psi_1^{-1}(p) - \sqrt{\frac{3}{10}} \phi_2'(n) \psi_1^0(p) + \sqrt{\frac{1}{10}} \phi_2^0(n) \psi_1'(p)$$

$$c_5 = \sqrt{\frac{1}{10}} \psi_1'(n) \phi_2^0(p) - \sqrt{\frac{3}{10}} \psi_1^0(n) \phi_2'(p) + \sqrt{\frac{3}{5}} \psi_1^{-1}(n) \phi_2^2(p)$$

$$c_6 = \phi_0^0(n) \psi_1'(p)$$

$$c_7 = \psi_1'(n) \phi_0^0(p)$$

$$c_8 = \sqrt{\frac{2}{10}} \psi_2^2(n) \psi_2^{-1}(p) - \sqrt{\frac{3}{10}} \psi_2'(n) \psi_2^0(p) + \sqrt{\frac{3}{10}} \psi_2^0(n) \psi_2'(p) - \sqrt{\frac{2}{10}} \psi_2^{-1}(n) \psi_2^2(p)$$

$$c_9 = \sqrt{\frac{3}{5}} \psi_2^2(n) \psi_1^{-1}(p) - \sqrt{\frac{3}{10}} \psi_2'(n) \psi_1^0(p) + \sqrt{\frac{1}{10}} \psi_2^0(n) \psi_1'(p)$$

$$c_{10} = \sqrt{\frac{1}{10}} \psi_1'(n) \psi_2^0(p) - \sqrt{\frac{3}{10}} \psi_1^0(n) \psi_2'(p) + \sqrt{\frac{3}{5}} \psi_1^{-1}(n) \psi_2^2(p)$$

$$c_{11} = \sqrt{\frac{1}{2}} \psi_1'(n) \psi_1^0(p) - \sqrt{\frac{1}{2}} \psi_1^0(n) \psi_1'(p)$$

$$c_{12} = \psi_1'(n) \xi_0^0(p)$$

$$c_{13} = \xi_0^0(n) \psi_1'(p)$$

One thing to notice about these wave functions is that a state in  $\text{Be}^8$ , formed solely from those having the configurations  $(1p_{3/2})^2 (1p_{1/2})^2$  and  $(1p_{3/2}) (1p_{1/2})^3$ , cannot be formed from  $\text{Li}^7$  having a configuration  $(1p_{3/2})^3$  by bombarding the  $\text{Li}^7$  with protons.

We now wish to assemble the 13 wave functions in linear

combinations which are eigenfunctions of the total isotopic spin. As in the case of the three particle wave functions, an operator  $\mathcal{T}^2$  may be found which is equivalent to  $T^2$ . It cannot, of course, be the same one as there is now an extra particle.

Let  $f(\overline{1234})$  be one of the four particle wave functions. Then we construct

$$\begin{aligned} F(\overline{1234}) &= (I - P_{14} - P_{24} - P_{34})(I - P_{13} - P_{23})f(\overline{1234})n(1)n(2)p(3)p(4) \\ &= 2(I + P_{13}P_{24} - P_{13} - P_{23} - P_{14} - P_{24})f(\overline{1234})n(1)n(2)p(3)p(4) \end{aligned}$$

and operate on it with  $T^2$  getting

$$\begin{aligned} T^2 F(\overline{1234}) &= 2n(1)n(2)p(3)p(4)(2I - P_{13} - P_{23} - P_{14} - P_{24})f(\overline{1234}) \\ &\quad + \text{other similar terms.} \end{aligned}$$

As before, we recognize that  $\mathcal{T}^2 = 2I - P_{13} - P_{23} - P_{14} - P_{24}$  operating on  $f(\overline{1234})$  is completely equivalent to  $T^2$  operating on  $F(\overline{1234})$ .

Corresponding to the possible values of the isotopic spin of 0, 1, and 2 for four particle wave functions,  $T^2$  and  $\mathcal{T}^2$  have eigenvalues, 0, 2, and 6. This fact can be used to construct projection operators for the three isotopic spins :

$$\Pi_0 = \frac{1}{12} (\mathcal{T}^2 - 6)(\mathcal{T}^2 - 2) = \frac{1}{6} (2I + 2P_{13}P_{24} + P_{13} + P_{23} + P_{14} + P_{24}) ,$$

$$\Pi_1 = \frac{1}{8} (6 - \mathcal{T}^2)\mathcal{T}^2 = \frac{1}{2} (I - P_{13}P_{24}) ,$$

$$\Pi_2 = \frac{1}{24} (\mathcal{T}^2 - 2)\mathcal{T}^2 = \frac{1}{6} (I + P_{13}P_{24} - P_{13} - P_{23} - P_{14} - P_{24}) .$$

Of these  $\Pi_1$  is of particular interest because of its simple form.

The operator  $P_{13}P_{24}$  interchanges neutrons and protons in a four particle wave function  $f(\overline{1234})$ . If this results in the function changing sign then  $\Pi_1 f = f$  and the function has  $T = 1$ . If the function is unchanged by  $P_{13}P_{24}$  then  $\Pi_1 f = 0$  and the function has no  $T = 1$  component. Actually,  $P_{13}P_{24}$  changes the functions  $C_1, C_2, C_3, \dots, C_{13}$  into one another so that we are led to the following linear combinations which have the required property :

$$\begin{aligned}
 D_1 &= C_1 & D_7 &= C_8 \\
 D_2 &= \sqrt{\frac{1}{2}} (C_2 - C_3) & D_8 &= C_{11} \\
 D_3 &= \sqrt{\frac{1}{2}} (C_4 - C_5) & D_9 &= \sqrt{\frac{1}{2}} (C_2 + C_3) \\
 D_4 &= \sqrt{\frac{1}{2}} (C_6 - C_7) & D_{10} &= \sqrt{\frac{1}{2}} (C_4 + C_5) \\
 D_5 &= \sqrt{\frac{1}{2}} (C_9 - C_{10}) & D_{11} &= \sqrt{\frac{1}{2}} (C_6 + C_7) \\
 D_6 &= \sqrt{\frac{1}{2}} (C_{12} - C_{13}) & D_{12} &= \sqrt{\frac{1}{2}} (C_9 + C_{10}) \\
 D_{13} &= \sqrt{\frac{1}{2}} (C_{12} + C_{13}) .
 \end{aligned}$$

$D_1$  through  $D_8$  change sign on the interchange of neutrons and protons while  $D_9$  through  $D_{13}$  are left unchanged. Thus

$$\begin{aligned}
 \Pi_1 D_i &= D_i & i &= 1, 2, \dots, 8 \\
 &= 0 & i &= 9, 10, \dots, 13.
 \end{aligned}$$

The first eight have  $T = 1$ , and the last five have only even isotopic spin components.

To find the linear combinations of  $D_9, D_{10}, \dots, D_{13}$  that are eigenfunctions of  $\mathcal{T}^2$ , we must find the eigenvectors of its matrix.

As in the case of  $Li^7$ , the work is simplified by the fact that the matrix elements of the different permutation operators are the same. The matrix of  $\tau^2$  is found to be

$$\tau^2 = \begin{pmatrix} \frac{5}{2} & \frac{5}{2} & -\frac{\sqrt{5}}{2} & 0 & 0 \\ \frac{5}{2} & \frac{5}{2} & -\frac{\sqrt{5}}{2} & 0 & 0 \\ -\frac{\sqrt{5}}{2} & -\frac{\sqrt{5}}{2} & 1 & 0 & 0 \\ 0 & 0 & 0 & 0 & 0 \\ 0 & 0 & 0 & 0 & 0 \end{pmatrix}$$

Its eigenvalues and eigenvectors are

$$\tau^2=6 \begin{pmatrix} \sqrt{\frac{5}{12}} \\ \sqrt{\frac{5}{12}} \\ -\sqrt{\frac{1}{6}} \\ 0 \\ 0 \end{pmatrix}, \tau^2=0 \begin{pmatrix} \sqrt{\frac{1}{12}} \\ \sqrt{\frac{1}{12}} \\ \sqrt{\frac{5}{6}} \\ 0 \\ 0 \end{pmatrix}, \tau^2=0 \begin{pmatrix} \sqrt{\frac{1}{2}} \\ -\sqrt{\frac{1}{2}} \\ 0 \\ 0 \\ 0 \end{pmatrix}, \tau^2=0 \begin{pmatrix} 0 \\ 0 \\ 0 \\ 1 \\ 0 \end{pmatrix}, \tau^2=0 \begin{pmatrix} 0 \\ 0 \\ 0 \\ 0 \\ 1 \end{pmatrix}$$

The corresponding wave functions are

$$E_2 = \sqrt{\frac{5}{12}} D_9 + \sqrt{\frac{5}{12}} D_{10} - \sqrt{\frac{1}{6}} D_{11}$$

$$E_6 = \sqrt{\frac{1}{12}} D_9 + \sqrt{\frac{1}{12}} D_{10} + \sqrt{\frac{5}{6}} D_{11}$$

$$E_7 = \sqrt{\frac{1}{2}} D_9 - \sqrt{\frac{1}{2}} D_{10}$$

$$E_{11} = D_{12}$$

$$E_{13} = D_{13}$$

It will be convenient for later calculations to take new linear combinations of the  $T = 1$  states so that they resemble the even  $T$  states. We set down as the final result for the  $jj$  coupling states of  $\text{Be}^8$  having  $J = 1^+$  the following functions :

$E_1 = C_1$	$T = 1$	$(1p_{3/2})^4$
$E_2 = \sqrt{\frac{5}{24}} (C_2 + C_3 + C_4 + C_5) - \sqrt{\frac{2}{24}} (C_6 + C_7)$	$= 2$	}
$E_3 = \sqrt{\frac{1}{24}} (C_2 - C_3 + C_4 - C_5) + \sqrt{\frac{10}{24}} (C_6 - C_7)$	$= 1$	
$E_4 = \sqrt{\frac{1}{4}} (C_2 - C_3 - C_4 + C_5)$	$= 1$	
$E_5 = \sqrt{\frac{5}{24}} (C_2 - C_3 + C_4 - C_5) - \sqrt{\frac{2}{24}} (C_6 - C_7)$	$= 1$	
$E_6 = \sqrt{\frac{1}{24}} (C_2 + C_3 + C_4 + C_5) + \sqrt{\frac{10}{24}} (C_6 + C_7)$	$= 0$	
$E_7 = \sqrt{\frac{1}{4}} (C_2 + C_3 - C_4 - C_5)$	$= 0$	
$E_8 = C_8$	$= 1$	
$E_9 = \sqrt{\frac{1}{2}} (C_9 - C_{10})$	$= 1$	
$E_{10} = C_{11}$	$= 1$	
$E_{11} = \sqrt{\frac{1}{2}} (C_9 + C_{10})$	$= 0$	
$E_{12} = \sqrt{\frac{1}{2}} (C_{12} - C_{13})$	$= 1$	}
$E_{13} = \sqrt{\frac{1}{2}} (C_{12} + C_{13})$	$= 0$	

$(1p_{3/2})^3(1p_{1/2})$   
 $(1p_{3/2})^2(1p_{1/2})^2$   
 $(1p_{3/2})(1p_{1/2})^3$

A.4.  $J = 0^+$  Wave Functions for  $\text{Be}^8$

In computing the probability of radiative capture of protons by  $\text{Li}^7$ , knowledge of the ground state wave function of  $\text{Be}^8$  is needed. This state has zero spin and isotopic spin and is expected, on the basis of the  $jj$  coupling model, to belong to the configuration  $(1p_{3/2})^4$ . There are two wave functions with zero spin and this configuration which are given in Table 6.

Table 6

$J = 0^+$  Wave Functions

	neutrons			protons			J
	$j_1$	$j_2$	$J_n$	$j_3$	$j_4$	$J_p$	
$F_1$	3/2	3/2	2	3/2	3/2	2	0
$F_2$	3/2	3/2	0	3/2	3/2	0	0

$$F_1 = \sqrt{\frac{1}{5}} \phi_2^2(n) \phi_2^{-2}(p) - \sqrt{\frac{1}{5}} \phi_2^1(n) \phi_2^1(p) + \sqrt{\frac{1}{5}} \phi_2^0(n) \phi_2^0(p) - \sqrt{\frac{1}{5}} \phi_2^{-1}(n) \phi_2^{-1}(p) + \sqrt{\frac{1}{5}} \phi_2^{-2}(n) \phi_2^{-2}(p)$$

$$F_0 = \phi_0^0(n) \phi_0^0(p)$$

On inspecting these wave functions, it is seen that both go into themselves on the interchange of neutrons and protons, so they can have no  $T = 1$  components. The matrix of  $\tau^2$  is calculated to be

$$\tau^2 = \begin{pmatrix} 5 & -\sqrt{5} \\ -\sqrt{5} & 1 \end{pmatrix}$$

which has as eigenvalues and eigenvectors

$$\tau^2 = 0 \begin{pmatrix} \sqrt{\frac{1}{6}} \\ \sqrt{\frac{5}{6}} \end{pmatrix}, \quad \tau^2 = 6 \begin{pmatrix} \sqrt{\frac{5}{6}} \\ -\sqrt{\frac{1}{6}} \end{pmatrix}.$$

The corresponding wave functions are

$$G_1 = \sqrt{\frac{1}{6}} F_1 + \sqrt{\frac{5}{6}} F_2 \quad T = 0,$$

$$G_2 = \sqrt{\frac{5}{6}} F_1 - \sqrt{\frac{1}{6}} F_2 \quad T = 2.$$

$G_1$  is the wave function for the ground state of  $\text{Be}^8$  in the  $jj$  coupling scheme.

#### A.5. Channel Spin Wave Functions

In computing scattering or reaction cross sections according to Wigner's theory of resonance reactions, it is necessary to have the wave function in that part of the configuration space where one of the particles (the incoming or outgoing one) is sufficiently separated from the rest, so that its interaction with the others involves at most Coulomb forces. These "channel spin" wave functions are constructed from the wave function of the bombarded (or residual) nucleus in its initial (or final) state and the wave function of the other particle in terms of relative coordinates. It is convenient to construct these functions as eigenfunctions of the relative angular momentum  $-\underline{l}^2$ , the channel spin  $-(\underline{I} + \underline{s})^2$ , and the total angular momentum  $-\underline{J}^2$ . ( $I$  is the angular momentum of the bombarded nucleus and  $s$  the spin of the bombarding particle.)



It is required, of course, that the channel spin wave functions be antisymmetric in the two protons as well as the two neutrons of the target nucleus. This can be achieved by coupling the spin and orbit of the bombarding proton to the angular momentum of the target nucleus as indicated in Table 7 and then antisymmetrizing by application of the operator  $\sqrt{\frac{1}{2}} (I - P_{34})$ . The factor  $\sqrt{\frac{1}{2}}$  gives the correct normalization: that is, with it the wave function has the same flux of particles at large radii as before antisymmetrization.

The channel spin wave functions for  $\text{Li}^7$  in its ground state ( $B_1$ ) and in its first excited state ( $A_3$ ) are needed and are listed in Table 7 being designated  $X_2^1$ ,  $X_1^1$ ,  $Z_1^1$ , and  $Z_0^1$ . The subscripts refer to the value of the channel spin.

Table 7

Channel Spin Wave Functions

$\text{Li}^7$  in Ground State

$$W_2^2 = B_1^{3/2}(123) \alpha(4)$$

$$W_2^1 = \sqrt{\frac{1}{4}} B_1^{3/2}(123) \beta(4) + \sqrt{\frac{3}{4}} B_1^{1/2}(123) \alpha(4)$$

$$W_2^0 = \sqrt{\frac{1}{2}} B_1^{1/2}(123) \beta(4) + \sqrt{\frac{1}{2}} B_1^{-1/2}(123) \alpha(4)$$

$$W_2^{-1} = \sqrt{\frac{3}{4}} B_1^{-1/2}(123) \beta(4) + \sqrt{\frac{1}{4}} B_1^{-3/2}(123) \alpha(4)$$

$$W_2^{-2} = B_1^{-3/2}(123) \beta(4)$$

Table 7 (continued)

Li<sup>7</sup> in Ground State

$$W_1^1 = \sqrt{\frac{3}{4}} B_1^{3/2}(123) \beta(4) - \sqrt{\frac{1}{4}} B_1^{1/2}(123) \alpha(4)$$

$$W_1^0 = \sqrt{\frac{1}{2}} B_1^{1/2}(123) \beta(4) - \sqrt{\frac{1}{2}} B_1^{-1/2}(123) \alpha(4)$$

$$W_1^{-1} = \sqrt{\frac{1}{4}} B_1^{-1/2}(123) \beta(4) - \sqrt{\frac{3}{4}} B_1^{-3/2}(123) \alpha(4)$$

$$X_2^1 = \sqrt{\frac{1}{2}} (I - P_{34}) \left[ \sqrt{\frac{3}{5}} W_2^1 Y_1^{-1}(4) - \sqrt{\frac{3}{10}} W_2^1 Y_1^0(4) + \sqrt{\frac{1}{10}} W_2^0 Y_1^1(4) \right]$$

$$X_1^1 = \sqrt{\frac{1}{2}} (I - P_{34}) \left[ \sqrt{\frac{1}{2}} W_1^1 Y_1^0(4) - \sqrt{\frac{1}{2}} W_1^0 Y_1^1(4) \right]$$

Li<sup>7</sup> in Excited State

$$U_1^1 = A_3^{1/2}(123) \alpha(4)$$

$$U_1^0 = \sqrt{\frac{1}{2}} A_3^{1/2}(123) \beta(4) + \sqrt{\frac{1}{2}} A_3^{-1/2}(123) \alpha(4)$$

$$U_1^{-1} = A_3^{-1/2}(123) \beta(4)$$

$$U_0^0 = \sqrt{\frac{1}{2}} A_3^{1/2}(123) \beta(4) - \sqrt{\frac{1}{2}} A_3^{-1/2}(123) \alpha(4)$$

$$Z_1^1 = \sqrt{\frac{1}{2}} (I - P_{34}) \left[ \sqrt{\frac{1}{2}} U_1^1 Y_1^0(4) - \sqrt{\frac{1}{2}} U_1^0 Y_1^1(4) \right]$$

$$Z_0^1 = \sqrt{\frac{1}{2}} (I - P_{34}) U_0^0 Y_1^1(4)$$

B. Wave Functions for LS Coupling Model

The construction of wave functions for Li<sup>7</sup> and Be<sup>8</sup> according to the LS (Russell - Saunders) coupling scheme is achieved in a

manner very similar to that used for the jj wave functions. The radial, angular, and spin wave functions are the same as before, but the order in which the angular momenta are added is different, so that our final wave functions have as quantum numbers L, S, J, and T.

The first step in building the wave functions needed is to construct two particle orbital and spin functions. These are listed in Table 8 with the symmetry or antisymmetry explicitly exhibited. It is to be understood, as in the case of the jj wave functions, that the orbital wave functions also contain the radial functions.

Table 8

Two Particle Orbital and Spin Functions

$$y_2^2(\overline{12}) = y_1^1(1)y_1^1(2)$$

$$y_2^1(\overline{12}) = \sqrt{\frac{1}{2}} y_1^1(1)y_1^0(2) + \sqrt{\frac{1}{2}} y_1^0(1)y_1^1(2)$$

$$y_2^0(\overline{12}) = \sqrt{\frac{1}{6}} y_1^1(1)y_1^{-1}(2) + \sqrt{\frac{2}{3}} y_1^0(1)y_1^0(2) + \sqrt{\frac{1}{6}} y_1^{-1}(1)y_1^1(2)$$

$$y_2^{-1}(\overline{12}) = \sqrt{\frac{1}{2}} y_1^0(1)y_1^{-1}(2) + \sqrt{\frac{1}{2}} y_1^{-1}(1)y_1^0(2)$$

$$y_2^{-2}(\overline{12}) = y_1^{-1}(1)y_1^{-1}(2)$$

$$y_1^1(\overline{12}) = \sqrt{\frac{1}{2}} y_1^1(1)y_1^0(2) - \sqrt{\frac{1}{2}} y_1^0(1)y_1^1(2)$$

$$y_1^0(\overline{12}) = \sqrt{\frac{1}{2}} y_1^1(1)y_1^{-1}(2) - \sqrt{\frac{1}{2}} y_1^{-1}(1)y_1^1(2)$$

$$y_1^{-1}(\overline{12}) = \sqrt{\frac{1}{2}} y_1^0(1)y_1^{-1}(2) - \sqrt{\frac{1}{2}} y_1^{-1}(1)y_1^0(2)$$

$$y_0^0(\overline{12}) = \sqrt{\frac{1}{3}} y_1^1(1)y_1^{-1}(2) - \sqrt{\frac{1}{3}} y_1^0(1)y_1^0(2) + \sqrt{\frac{1}{3}} y_1^{-1}(1)y_1^1(2)$$

Table 8 (continued)

$$\chi_1^1(\bar{12}) = \chi_{\frac{1}{2}}^{\frac{1}{2}}(1) \chi_{\frac{1}{2}}^{\frac{1}{2}}(2)$$

$$\chi_1^0(\bar{12}) = \sqrt{\frac{1}{2}} \chi_{\frac{1}{2}}^{\frac{1}{2}}(1) \chi_{\frac{1}{2}}^{-\frac{1}{2}}(2) + \sqrt{\frac{1}{2}} \chi_{\frac{1}{2}}^{-\frac{1}{2}}(1) \chi_{\frac{1}{2}}^{\frac{1}{2}}(2)$$

$$\chi_1^{-1}(\bar{12}) = \chi_{\frac{1}{2}}^{\frac{1}{2}}(1) \chi_{\frac{1}{2}}^{-\frac{1}{2}}(2)$$

$$\chi_0^0(\bar{12}) = \sqrt{\frac{1}{2}} \chi_{\frac{1}{2}}^{\frac{1}{2}}(1) \chi_{\frac{1}{2}}^{\frac{1}{2}}(2) - \sqrt{\frac{1}{2}} \chi_{\frac{1}{2}}^{-\frac{1}{2}}(1) \chi_{\frac{1}{2}}^{-\frac{1}{2}}(2)$$

Since there is the requirement of antisymmetry on wave functions of identical particles, we must restrict ourselves to the following combinations of  $L_n$  and  $S_n$  :

$L_n$	$S_n$
2	0
0	0
1	0

In the case of  $\text{Be}^8$ , where there are two protons as well as two neutrons, the same values of  $L_p$  and  $S_p$  are allowed.

From the two particle orbital and spin wave functions in Table 8 three and four particle orbital and spin wave functions are formed. These are listed in Tables 9 and 10.

### B.1. $J = 3/2^-$ Wave Functions for $\text{Li}^7$

The spin of  $\text{Li}^7$  in its ground state is, as noted previously,  $3/2$  and the parity odd. Eight wave functions having this spin and

parity can be constructed from 1p single particle wave functions. They are listed together with their spectroscopic designations in Table 11. The reason for there being more than in the case of jj coupling (where only two were considered) is that the whole 1p shell is being used and not just a sub-shell as in that case.

Table 9

Three Particle Orbital and Spin Functions

$$y_2^2(\bar{1}23) = \sqrt{\frac{2}{3}} y_2^2(\bar{1}2) Y_1^0(3) - \sqrt{\frac{1}{3}} y_2^1(12) Y_1^1(3)$$

$$y_2^1(\bar{1}23) = \sqrt{\frac{1}{3}} y_2^2(12) Y_1^{-1}(3) + \sqrt{\frac{1}{6}} y_2^1(12) Y_1^0(3) - \sqrt{\frac{1}{2}} y_2^0(12) Y_1^1(3)$$

$$y_2^0(\bar{1}23) = \sqrt{\frac{1}{2}} y_2^1(12) Y_1^{-1}(3) - \sqrt{\frac{1}{2}} y_2^1(12) Y_1^1(3)$$

$$y_2^{-1}(\bar{1}23) = \sqrt{\frac{1}{2}} y_2^0(12) Y_1^{-1}(3) - \sqrt{\frac{1}{6}} y_2^1(12) Y_1^0(3) - \sqrt{\frac{1}{3}} y_2^2(12) Y_1^1(3)$$

$$y_2^{-2}(\bar{1}23) = \sqrt{\frac{1}{3}} y_2^1(12) Y_1^{-1}(3) - \sqrt{\frac{2}{3}} y_2^2(12) Y_1^0(3)$$

$$y_1^1(\bar{1}23) = \sqrt{\frac{3}{5}} y_2^2(12) Y_1^{-1}(3) - \sqrt{\frac{3}{10}} y_2^1(12) Y_1^0(3) + \sqrt{\frac{1}{10}} y_2^0(12) Y_1^1(3)$$

$$y_1^0(\bar{1}23) = \sqrt{\frac{3}{10}} y_2^1(12) Y_1^{-1}(3) - \sqrt{\frac{2}{5}} y_2^0(12) Y_1^0(3) + \sqrt{\frac{3}{10}} y_2^1(12) Y_1^1(3)$$

$$y_1^{-1}(\bar{1}23) = \sqrt{\frac{1}{10}} y_2^0(12) Y_1^{-1}(3) - \sqrt{\frac{3}{10}} y_2^1(12) Y_1^0(3) + \sqrt{\frac{3}{5}} y_2^2(12) Y_1^1(3)$$

$$y_2^2(\bar{1}\bar{2}3) = y_1^1(12) Y_1^1(3)$$

$$y_2^1(\bar{1}\bar{2}3) = \sqrt{\frac{1}{2}} y_1^1(12) Y_1^0(3) + \sqrt{\frac{1}{2}} y_1^0(12) Y_1^1(3)$$

$$y_2^0(\bar{1}\bar{2}3) = \sqrt{\frac{1}{6}} y_1^1(12) Y_1^{-1}(3) + \sqrt{\frac{2}{3}} y_1^0(12) Y_1^0(3) + \sqrt{\frac{1}{6}} y_1^{-1}(12) Y_1^1(3)$$

$$y_2^{-1}(\bar{1}\bar{2}3) = \sqrt{\frac{1}{2}} y_1^0(12) Y_1^{-1}(3) + \sqrt{\frac{1}{2}} y_1^{-1}(12) Y_1^0(3)$$

Table 9 (continued)

$$y_2^{\overline{123}} = y_1^{\overline{12}} y_1^{-1}(3)$$

$$y_1^{\overline{123}} = \sqrt{\frac{1}{2}} y_1^{\overline{12}} y_1^0(3) - \sqrt{\frac{1}{2}} y_1^0(12) y_1^{\overline{123}}$$

$$y_1^0(\overline{123}) = \sqrt{\frac{1}{2}} y_1^{\overline{12}} y_1^{-1}(3) - \sqrt{\frac{1}{2}} y_1^{-1}(12) y_1^{\overline{123}}$$

$$y_1^{-1}(\overline{123}) = \sqrt{\frac{1}{2}} y_1^0(12) y_1^{-1}(3) - \sqrt{\frac{1}{2}} y_1^{-1}(12) y_1^0(3)$$

$$y_0^0(\overline{123}) = \sqrt{\frac{1}{3}} y_1^{\overline{12}} y_1^{-1}(3) - \sqrt{\frac{1}{3}} y_1^0(12) y_1^0(3) + \sqrt{\frac{1}{3}} y_1^{-1}(12) y_1^{\overline{123}}$$

$$\tilde{y}_1^{\overline{123}} = y_0^0(12) y_1^{\overline{123}}$$

$$\tilde{y}_1^0(\overline{123}) = y_0^0(12) y_1^0(3)$$

$$\tilde{y}_1^{-1}(\overline{123}) = y_0^0(12) y_1^{-1}(3)$$

$$\chi_{3/2}^{\overline{123}} = \chi_1^{\overline{12}} \chi_{1/2}^{\overline{123}}$$

$$\chi_{3/2}^{\overline{123}} = \sqrt{\frac{1}{3}} \chi_1^{\overline{12}} \chi_{1/2}^{-1/2}(3) + \sqrt{\frac{2}{3}} \chi_1^0(12) \chi_{1/2}^{\overline{123}}$$

$$\chi_{3/2}^{-1/2}(\overline{123}) = \sqrt{\frac{2}{3}} \chi_1^0(12) \chi_{1/2}^{-1/2}(3) + \sqrt{\frac{1}{3}} \chi_1^{-1}(12) \chi_{1/2}^{\overline{123}}$$

$$\chi_{3/2}^{-3/2}(\overline{123}) = \chi_1^{-1}(12) \chi_{1/2}^{-1/2}(3)$$

$$\chi_{1/2}^{\overline{123}} = \sqrt{\frac{2}{3}} \chi_1^{\overline{12}} \chi_{1/2}^{-1/2}(3) - \sqrt{\frac{1}{3}} \chi_1^0(12) \chi_{1/2}^{\overline{123}}$$

$$\chi_{1/2}^{-1/2}(\overline{123}) = \sqrt{\frac{1}{3}} \chi_1^0(12) \chi_{1/2}^{-1/2}(3) - \sqrt{\frac{2}{3}} \chi_1^{-1}(12) \chi_{1/2}^{\overline{123}}$$

Table 9 (continued)

$$\chi_{\frac{1}{2}}^{\frac{1}{2}}(\bar{1}\bar{2}\bar{3}) = \chi_0^0(12) \chi_{\frac{1}{2}}^{\frac{1}{2}}(3)$$

$$\chi_{\frac{1}{2}}^{-\frac{1}{2}}(\bar{1}\bar{2}\bar{3}) = \chi_0^0(12) \chi_{\frac{1}{2}}^{-\frac{1}{2}}(3)$$

Table 10

Four Particle Orbital and Spin Functions

$$y_1'(\bar{1}\bar{2}\bar{3}\bar{4}) = \sqrt{\frac{2}{10}} y_2^2(12) y_2^{-1}(34) - \sqrt{\frac{3}{10}} y_2'(12) y_2^0(34) + \sqrt{\frac{3}{10}} y_2^0(12) y_2'(34) - \sqrt{\frac{2}{10}} y_2^{-1}(12) y_2^2(34)$$

$$y_1^0(\bar{1}\bar{2}\bar{3}\bar{4}) = \sqrt{\frac{4}{10}} y_2^2(12) y_2^{-2}(34) - \sqrt{\frac{1}{10}} y_2'(12) y_2^{-1}(34) + \sqrt{\frac{1}{10}} y_2^{-1}(12) y_2'(34) - \sqrt{\frac{4}{10}} y_2^{-2}(12) y_2^2(34)$$

$$y_1^{-1}(\bar{1}\bar{2}\bar{3}\bar{4}) = \sqrt{\frac{2}{10}} y_2'(12) y_2^{-2}(34) - \sqrt{\frac{3}{10}} y_2^0(12) y_2^{-1}(34) + \sqrt{\frac{3}{10}} y_2^{-1}(12) y_2^0(34) - \sqrt{\frac{2}{10}} y_2^{-2}(12) y_2'(34)$$

$$y_2^2(\bar{1}\bar{2}\bar{3}\bar{4}) = \sqrt{\frac{2}{3}} y_2^2(12) y_1^0(34) - \sqrt{\frac{1}{3}} y_2'(12) y_1'(34)$$

$$y_2^1(\bar{1}\bar{2}\bar{3}\bar{4}) = \sqrt{\frac{1}{3}} y_2^2(12) y_1^{-1}(34) + \sqrt{\frac{1}{6}} y_2'(12) y_1^0(34) - \sqrt{\frac{1}{2}} y_2^0(12) y_1'(34)$$

$$y_2^0(\bar{1}\bar{2}\bar{3}\bar{4}) = \sqrt{\frac{1}{2}} y_2'(12) y_1^{-1}(34) - \sqrt{\frac{1}{2}} y_2^{-1}(12) y_1'(34)$$

$$y_2^{-1}(\bar{1}\bar{2}\bar{3}\bar{4}) = \sqrt{\frac{1}{2}} y_2^0(12) y_1^{-1}(34) - \sqrt{\frac{1}{6}} y_2^{-1}(12) y_1^0(34) - \sqrt{\frac{1}{3}} y_2^{-2}(12) y_1'(34)$$

$$y_2^{-2}(\bar{1}\bar{2}\bar{3}\bar{4}) = \sqrt{\frac{1}{3}} y_2^{-1}(12) y_1^{-1}(34) - \sqrt{\frac{2}{3}} y_2^{-2}(12) y_1^0(34)$$

$$y_1'(\bar{1}\bar{2}\bar{3}\bar{4}) = \sqrt{\frac{3}{5}} y_2^2(12) y_1^{-1}(34) - \sqrt{\frac{3}{10}} y_2'(12) y_1^0(34) + \sqrt{\frac{1}{10}} y_2^0(12) y_1'(34)$$

$$y_1^0(\bar{1}\bar{2}\bar{3}\bar{4}) = \sqrt{\frac{3}{10}} y_2'(12) y_1^{-1}(34) - \sqrt{\frac{2}{5}} y_2^0(12) y_1^0(34) + \sqrt{\frac{3}{10}} y_2^{-1}(12) y_1'(34)$$

$$y_1^{-1}(\bar{1}\bar{2}\bar{3}\bar{4}) = \sqrt{\frac{1}{10}} y_2^0(12) y_1^{-1}(34) - \sqrt{\frac{3}{10}} y_2^{-1}(12) y_1^0(34) + \sqrt{\frac{3}{5}} y_2^{-2}(12) y_1'(34)$$

$$y_2^2(\bar{1}\bar{2}\bar{3}\bar{4}) = y_1'(12) y_1'(34)$$

$$y_2^1(\bar{1}\bar{2}\bar{3}\bar{4}) = \sqrt{\frac{1}{2}} y_1'(12) y_1^0(34) + \sqrt{\frac{1}{2}} y_1^0(12) y_1'(34)$$

Table 10 (continued)

$$y_2^0(\overline{1234}) = \sqrt{\frac{1}{6}} y_1'(12) y_1^{-1}(34) + \sqrt{\frac{2}{3}} y_1^0(12) y_1^0(34) + \sqrt{\frac{1}{6}} y_1^{-1}(12) y_1'(34)$$

$$y_2^{-1}(\overline{1234}) = \sqrt{\frac{1}{2}} y_1^0(12) y_1^{-1}(34) + \sqrt{\frac{1}{2}} y_1^{-1}(12) y_1^0(34)$$

$$y_2^{-2}(\overline{1234}) = y_1^{-1}(12) y_1^{-1}(34)$$

$$y_1'(1234) = \sqrt{\frac{1}{2}} y_1'(12) y_1^0(34) - \sqrt{\frac{1}{2}} y_1^0(12) y_1'(34)$$

$$y_1^0(1234) = \sqrt{\frac{1}{2}} y_1'(12) y_1^{-1}(34) - \sqrt{\frac{1}{2}} y_1^{-1}(12) y_1'(34)$$

$$y_1^{-1}(1234) = \sqrt{\frac{1}{2}} y_1^0(12) y_1^{-1}(34) - \sqrt{\frac{1}{2}} y_1^{-1}(12) y_1^0(34)$$

$$y_0^0(\overline{1234}) = \sqrt{\frac{1}{3}} y_1'(12) y_1^{-1}(34) - \sqrt{\frac{1}{3}} y_1^0(12) y_1^0(34) + \sqrt{\frac{1}{3}} y_1^{-1}(12) y_1'(34)$$

$$\tilde{y}_1'(1234) = y_1'(12) y_0^0(34)$$

$$\tilde{y}_1^0(1234) = y_1^0(12) y_0^0(34)$$

$$\tilde{y}_1^{-1}(1234) = y_1^{-1}(12) y_0^0(34)$$

$$\chi_2^2(\overline{1234}) = \chi_1'(12) \chi_1'(34)$$

$$\chi_2^1(\overline{1234}) = \sqrt{\frac{1}{2}} \chi_1'(12) \chi_1^0(34) + \sqrt{\frac{1}{2}} \chi_1^0(12) \chi_1'(34)$$

$$\chi_2^0(\overline{1234}) = \sqrt{\frac{1}{6}} \chi_1'(12) \chi_1^{-1}(34) + \sqrt{\frac{2}{3}} \chi_1^0(12) \chi_1^0(34) + \sqrt{\frac{1}{6}} \chi_1^{-1}(12) \chi_1'(34)$$

$$\chi_2^{-1}(\overline{1234}) = \sqrt{\frac{1}{2}} \chi_1^0(12) \chi_1^{-1}(34) + \sqrt{\frac{1}{2}} \chi_1^{-1}(12) \chi_1^0(34)$$

$$\chi_2^{-2}(\overline{1234}) = \chi_1^{-1}(12) \chi_1^{-1}(34)$$

$$\chi_1'(1234) = \sqrt{\frac{1}{2}} \chi_1'(12) \chi_1^0(34) - \sqrt{\frac{1}{2}} \chi_1^0(12) \chi_1'(34)$$



Table 10 (continued)

$$\begin{aligned} \chi_{1'(\bar{1}2\bar{3}4)}^{\circ} &= \sqrt{\frac{1}{2}} \chi_{1'(12)}^{\circ} \chi_{1'(34)}^{\circ} - \sqrt{\frac{1}{2}} \chi_{1'(12)}^{\circ} \chi_{1'(34)}^{\circ} \\ \chi_{1'(\bar{1}2\bar{3}4)}^{\circ} &= \sqrt{\frac{1}{2}} \chi_{1'(12)}^{\circ} \chi_{1'(34)}^{\circ} - \sqrt{\frac{1}{2}} \chi_{1'(12)}^{\circ} \chi_{1'(34)}^{\circ} \\ \chi_{0^{\circ}(\bar{1}2\bar{3}4)}^{\circ} &= \sqrt{\frac{1}{3}} \chi_{1'(12)}^{\circ} \chi_{1'(34)}^{\circ} - \sqrt{\frac{1}{3}} \chi_{1'(12)}^{\circ} \chi_{1'(34)}^{\circ} + \sqrt{\frac{1}{3}} \chi_{1'(12)}^{\circ} \chi_{1'(34)}^{\circ} \\ \chi_{1'(\bar{1}2\bar{3}4)}^{\circ} &= \chi_{1'(12)}^{\circ} \chi_{0^{\circ}(34)}^{\circ} \\ \chi_{1^{\circ}(\bar{1}2\bar{3}4)}^{\circ} &= \chi_{1^{\circ}(12)}^{\circ} \chi_{0^{\circ}(34)}^{\circ} \\ \chi_{1'(\bar{1}2\bar{3}4)}^{\circ} &= \chi_{1'(12)}^{\circ} \chi_{0^{\circ}(34)}^{\circ} \\ \chi_{0^{\circ}(\bar{1}2\bar{3}4)}^{\circ} &= \chi_{0^{\circ}(12)}^{\circ} \chi_{0^{\circ}(34)}^{\circ} \end{aligned}$$

Table 11

J = 3/2<sup>-</sup> Wave Functions

	L <sub>n</sub>	S <sub>n</sub>	L <sub>p</sub>	S <sub>p</sub>	L	S	J	
H <sub>1</sub>	1	1	1	1/2	2	3/2	3/2	<sup>4</sup> D <sub>3/2</sub>
H <sub>2</sub>	1	1	1	1/2	1	3/2	3/2	<sup>4</sup> P <sub>3/2</sub>
H <sub>3</sub>	1	1	1	1/2	0	3/2	3/2	<sup>4</sup> S <sub>3/2</sub>
H <sub>4</sub>	2	0	1	1/2	2	1/2	3/2	} <sup>2</sup> D <sub>3/2</sub>
H <sub>5</sub>	1	1	1	1/2	2	1/2	3/2	

Table 11 (continued)

	$L_n$	$S_n$	$L_p$	$S_p$	$L$	$S$	$J$
$H_6$	2	0	1	1/2	1	1/2	3/2
$H_7$	1	1	1	1/2	1	1/2	3/2
$H_8$	0	0	1	1/2	1	1/2	3/2

}  ${}^2P_{3/2}$

$$H_1^{3/2} = \sqrt{\frac{2}{5}} y_2^2(\bar{1}23) \chi_{3/2}^{-1/2}(\bar{1}23) - \sqrt{\frac{2}{5}} y_2'(\bar{1}23) \chi_{3/2}^{1/2}(\bar{1}23) + \sqrt{\frac{1}{5}} y_2^0(\bar{1}23) \chi_{3/2}^{3/2}(\bar{1}23)$$

$$H_2^{3/2} = \sqrt{\frac{3}{5}} y_1^0(\bar{1}23) \chi_{3/2}^{3/2}(\bar{1}23) - \sqrt{\frac{2}{5}} y_1'(\bar{1}23) \chi_{3/2}^{1/2}(\bar{1}23)$$

$$H_3^{3/2} = y_0^0(\bar{1}23) \chi_{3/2}^{3/2}(\bar{1}23)$$

$$H_4^{3/2} = \sqrt{\frac{4}{5}} y_2^2(\bar{1}23) \chi_{3/2}^{-1/2}(\bar{1}23) - \sqrt{\frac{1}{5}} y_2'(\bar{1}23) \chi_{3/2}^{1/2}(\bar{1}23)$$

$$H_5^{3/2} = \sqrt{\frac{4}{5}} y_2^2(\bar{1}23) \chi_{3/2}^{-1/2}(\bar{1}23) - \sqrt{\frac{1}{5}} y_2'(\bar{1}23) \chi_{3/2}^{1/2}(\bar{1}23)$$

$$H_6^{3/2} = y_1'(\bar{1}23) \chi_{3/2}^{1/2}(\bar{1}23)$$

$$H_7^{3/2} = y_1'(\bar{1}23) \chi_{3/2}^{1/2}(\bar{1}23)$$

$$H_8^{3/2} = \tilde{y}_1'(\bar{1}23) \chi_{3/2}^{1/2}(\bar{1}23)$$

The functions  $H_1, H_2, \dots, H_8$  may now be resolved into eigenfunctions of the isotopic spin exactly as before using  $\tau^2 = 7/4 I - P_{13} - P_{23}$  as the isotopic spin operator. This leads to the following eight functions :

$$\begin{array}{lll}
 K_1 = H_1 & T = 1/2 & {}^4D_{3/2} \\
 K_2 = H_2 & = 1/2 & {}^4P_{3/2} \\
 K_3 = H_3 & = 3/2 & {}^4S_{3/2} \\
 K_4 = \sqrt{\frac{1}{2}} (H_4 + H_5) & = 1/2 & \left. \vphantom{K_4} \right\} {}^2D_{3/2} \\
 K_5 = \sqrt{\frac{1}{2}} (H_4 - H_5) & = 3/2 & \\
 K_6 = \sqrt{\frac{5}{18}} H_6 + \sqrt{\frac{9}{18}} H_7 - \sqrt{\frac{4}{18}} H_8 & = 3/2 & \left. \vphantom{K_6} \right\} {}^2P_{3/2} \\
 K_7 = \sqrt{\frac{5}{18}} H_6 - \sqrt{\frac{9}{18}} H_7 - \sqrt{\frac{4}{18}} H_8 & = 1/2 & \\
 K_8 = \sqrt{\frac{4}{9}} H_6 + \sqrt{\frac{5}{9}} H_7 & = 1/2 & 
 \end{array}$$

It should be noted that  $K_7$  and  $K_8$  are degenerate so that other linear combinations of them might be chosen. As chosen here,  $K_8$  has a completely symmetric spatial wave function and is thus expected to have the lowest energy. It will be taken as the ground state wave function for  $\text{Li}^7$  in the LS coupling scheme. This choice is supported by the fact that the magnetic moment, calculated from  $K_8$  is fairly good, being 3.12 nuclear magnetons which is to be compared with the experimental value of 3.26 nuclear magnetons.

### B.2. $J = 1/2^-$ Wave Functions for $\text{Li}^7$

The first excited state of  $\text{Li}^7$  is known to have a spin of  $1/2$  and odd parity. The wave functions listed in Table 12 are of this type.

Table 12

J = 1/2<sup>-</sup> Wave Functions

	L <sub>n</sub>	S <sub>n</sub>	L <sub>p</sub>	S <sub>p</sub>	L	S	J	
H <sub>9</sub>	1	1	1	1/2	2	3/2	1/2	<sup>4</sup> D <sub>1/2</sub>
H <sub>10</sub>	1	1	1	1/2	1	3/2	1/2	<sup>4</sup> P <sub>1/2</sub>
H <sub>11</sub>	1	1	1	1/2	1	1/2	1/2	
H <sub>12</sub>	2	0	1	1/2	1	1/2	1/2	<sup>2</sup> P <sub>1/2</sub>
H <sub>13</sub>	0	0	1	1/2	1	1/2	1/2	
H <sub>14</sub>	1	1	1	1/2	0	1/2	1/2	<sup>2</sup> S <sub>1/2</sub>

$$H_9^{1/2} = \sqrt{\frac{2}{5}} y_2^1(\bar{1}23) \chi_{3/2}^{3/2}(\bar{1}23) - \sqrt{\frac{3}{10}} y_2^1(\bar{1}23) \chi_{3/2}^{-1/2}(\bar{1}23) + \sqrt{\frac{1}{5}} y_2^0(\bar{1}23) \chi_{3/2}^{1/2}(\bar{1}23) - \sqrt{\frac{1}{10}} y_2^{-1}(\bar{1}23) \chi_{3/2}^{3/2}(\bar{1}23)$$

$$H_{10}^{1/2} = \sqrt{\frac{1}{6}} y_1^1(\bar{1}23) \chi_{3/2}^{-1/2}(\bar{1}23) - \sqrt{\frac{1}{3}} y_1^0(\bar{1}23) \chi_{3/2}^{1/2}(\bar{1}23) + \sqrt{\frac{1}{2}} y_1^{-1}(\bar{1}23) \chi_{3/2}^{3/2}(\bar{1}23)$$

$$H_{11}^{1/2} = \sqrt{\frac{2}{3}} y_1^1(\bar{1}23) \chi_{1/2}^{-1/2}(\bar{1}23) - \sqrt{\frac{1}{3}} y_1^0(\bar{1}23) \chi_{1/2}^{1/2}(\bar{1}23)$$

$$H_{12}^{1/2} = \sqrt{\frac{2}{3}} y_1^1(\bar{1}23) \chi_{1/2}^{-1/2}(\bar{1}23) - \sqrt{\frac{1}{3}} y_1^0(\bar{1}23) \chi_{1/2}^{1/2}(\bar{1}23)$$

$$H_{13}^{1/2} = \sqrt{\frac{2}{3}} \tilde{y}_1^1(\bar{1}23) \chi_{1/2}^{-1/2}(\bar{1}23) - \sqrt{\frac{1}{3}} \tilde{y}_1^0(\bar{1}23) \chi_{1/2}^{1/2}(\bar{1}23)$$

$$H_{14}^{1/2} = y_0^0(\bar{1}23) \chi_{1/2}^{1/2}(\bar{1}23)$$

The appropriate linear combinations which are eigenfunctions of the isotopic spin are :

$$K_9 = H_9$$

$$T = 1/2 \quad {}^4D_{1/2}$$

$$K_{10} = H_{10}$$

$$T = 1/2 \quad {}^4P_{1/2}$$

$$K_{11} = \sqrt{\frac{9}{18}} H_{11} + \sqrt{\frac{5}{18}} H_{12} - \sqrt{\frac{4}{18}} H_{13}$$

$$T = 3/2$$

$$K_{12} = -\sqrt{\frac{9}{18}} H_{11} + \sqrt{\frac{5}{18}} H_{12} - \sqrt{\frac{4}{18}} H_{13}$$

$$T = 1/2$$

$$K_{13} = \sqrt{\frac{4}{9}} H_{12} + \sqrt{\frac{5}{9}} H_{13}$$

$$T = 1/2$$

$${}^2P_{1/2}$$

$$K_{14} = H_{14}$$

$$T = 1/2 \quad {}^2S_{1/2}$$

As in the case of the  ${}^2P_{3/2}$  states, there is a degeneracy in the  ${}^2P_{1/2}$ ,  $T = 1/2$  states. Any linear combination of  $K_{12}$  or  $K_{13}$  may be chosen but, as set down,  $K_{13}$  has complete spatial symmetry and should have a lower energy than any other of the states  $K_9, K_{10}, \dots, K_{14}$ . It will be chosen to represent the 478 kev state of  $Li^7$  in the LS coupling scheme.

### B.3. $J = 1^+$ Wave Functions for $Be^8$

The  $J = 1^+$  wave functions, which presumably include those of the 17.63 and 18.14 Mev states of  $Be^8$  in their number, are listed in Table 13. There are the same number of wave functions - thirteen - as in the case of jj coupling as is to be expected.

Table 13

J = 1<sup>+</sup> Wave Functions

	L <sub>N</sub>	S <sub>N</sub>	L <sub>P</sub>	S <sub>P</sub>	L	S	J	
N <sub>1</sub>	2	0	2	0	1	0	1	} 1P <sub>1</sub>
N <sub>2</sub>	1	1	1	1	1	0	1	
N <sub>3</sub>	1	1	1	1	0	1	1	3S <sub>1</sub>
N <sub>4</sub>	1	1	2	0	1	1	1	} 3P <sub>1</sub>
N <sub>5</sub>	2	0	1	1	1	1	1	
N <sub>6</sub>	1	1	1	1	1	1	1	
N <sub>7</sub>	1	1	0	0	1	1	1	
N <sub>8</sub>	0	0	1	1	1	1	1	
N <sub>9</sub>	1	1	2	0	2	1	1	} 3D <sub>1</sub>
N <sub>10</sub>	2	0	1	1	2	1	1	
N <sub>11</sub>	1	1	1	1	2	1	1	
N <sub>12</sub>	1	1	1	1	1	2	1	5P <sub>1</sub>
N <sub>13</sub>	1	1	1	1	2	2	1	5D <sub>1</sub>

$$N_1' = y_1'(\overline{1234}) \chi_0^\circ(\overline{1234})$$

$$N_2' = y_1'(\overline{1234}) \chi_0^\circ(\overline{1234})$$

$$N_3' = y_0^\circ(\overline{1234}) \chi_1'(\overline{1234})$$

$$N_4' = \frac{\sqrt{1}}{2} y_1'(\overline{1234}) \chi_1^\circ(\overline{1234}) - \frac{\sqrt{1}}{2} y_0^\circ(\overline{1234}) \chi_1'(\overline{1234})$$

Table 13 (continued)

$$\begin{aligned}
 N'_5 &= \sqrt{\frac{1}{2}} y'_1 (\bar{1}2\bar{3}4) \chi_1^0 (\bar{1}2\bar{3}4) - \sqrt{\frac{1}{2}} y_1^0 (\bar{1}2\bar{3}4) \chi_1' (\bar{1}2\bar{3}4) \\
 N'_6 &= \sqrt{\frac{1}{2}} y'_1 (\bar{1}2\bar{3}4) \chi_1^0 (\bar{1}2\bar{3}4) - \sqrt{\frac{1}{2}} y_1^0 (\bar{1}2\bar{3}4) \chi_1' (\bar{1}2\bar{3}4) \\
 N'_7 &= \sqrt{\frac{1}{2}} y'_1 (\bar{1}2\bar{3}4) \chi_1^0 (\bar{1}2\bar{3}4) - \sqrt{\frac{1}{2}} y_1^0 (\bar{1}2\bar{3}4) \chi_1' (\bar{1}2\bar{3}4) \\
 N'_8 &= \sqrt{\frac{1}{2}} y'_1 (\bar{1}2\bar{3}4) \chi_1^0 (\bar{1}2\bar{3}4) - \sqrt{\frac{1}{2}} y_1^0 (\bar{1}2\bar{3}4) \chi_1' (\bar{1}2\bar{3}4) \\
 N'_9 &= \sqrt{\frac{3}{5}} y_2' (\bar{1}2\bar{3}4) \chi_1' (\bar{1}2\bar{3}4) - \sqrt{\frac{3}{10}} y_1' (\bar{1}2\bar{3}4) \chi_1^0 (\bar{1}2\bar{3}4) + \sqrt{\frac{1}{10}} y_2^0 (\bar{1}2\bar{3}4) \chi_1' (\bar{1}2\bar{3}4) \\
 N'_{10} &= \sqrt{\frac{2}{5}} y_2' (\bar{1}2\bar{3}4) \chi_1' (\bar{1}2\bar{3}4) - \sqrt{\frac{3}{10}} y_1' (\bar{1}2\bar{3}4) \chi_1^0 (\bar{1}2\bar{3}4) + \sqrt{\frac{1}{10}} y_2^0 (\bar{1}2\bar{3}4) \chi_1' (\bar{1}2\bar{3}4) \\
 N'_{11} &= \sqrt{\frac{3}{5}} y_2' (\bar{1}2\bar{3}4) \chi_1' (\bar{1}2\bar{3}4) - \sqrt{\frac{3}{10}} y_1' (\bar{1}2\bar{3}4) \chi_1^0 (\bar{1}2\bar{3}4) + \sqrt{\frac{1}{10}} y_2^0 (\bar{1}2\bar{3}4) \chi_1' (\bar{1}2\bar{3}4) \\
 N'_{12} &= \sqrt{\frac{1}{10}} y_1' (\bar{1}2\bar{3}4) \chi_2^0 (\bar{1}2\bar{3}4) - \sqrt{\frac{3}{10}} y_1^0 (\bar{1}2\bar{3}4) \chi_2' (\bar{1}2\bar{3}4) + \sqrt{\frac{3}{5}} y_1' (\bar{1}2\bar{3}4) \chi_2^2 (\bar{1}2\bar{3}4) \\
 N'_{13} &= \sqrt{\frac{2}{10}} y_2' (\bar{1}2\bar{3}4) \chi_2' (\bar{1}2\bar{3}4) - \sqrt{\frac{3}{10}} y_1' (\bar{1}2\bar{3}4) \chi_2^0 (\bar{1}2\bar{3}4) + \sqrt{\frac{3}{10}} y_2^0 (\bar{1}2\bar{3}4) \chi_2' (\bar{1}2\bar{3}4) \\
 &\quad - \sqrt{\frac{2}{10}} y_1' (\bar{1}2\bar{3}4) \chi_2^2 (\bar{1}2\bar{3}4)
 \end{aligned}$$

From the matrix of the isotopic spin operator  $\tau^2 = 2I - P_{13} - P_{14} - P_{14} - P_{24}$  its eigenfunctions can be found. These are :

$P_1 = N_1$	$\tau = 1$	}	$1P_1$
$P_2 = N_2$	$= 1$		
$P_3 = N_3$	$= 1$		$3S_1$
$P_4 = \sqrt{\frac{5}{18}}(N_4 + N_5) - \sqrt{\frac{1}{3}}N_6 + \sqrt{\frac{1}{18}}(N_7 + N_8)$	$= 2$	}	$3P_1$
$P_5 = \sqrt{\frac{5}{12}}(N_4 - N_5) + \sqrt{\frac{1}{12}}(N_7 - N_8)$	$= 1$		
$P_6 = \sqrt{\frac{1}{12}}(N_4 - N_5) - \sqrt{\frac{5}{12}}(N_7 - N_8)$	$= 1$		
$P_7 = \sqrt{\frac{5}{36}}(N_4 + N_5) + \sqrt{\frac{2}{3}}N_6 + \sqrt{\frac{1}{36}}(N_7 + N_8)$	$= 0$		
$P_8 = \sqrt{\frac{1}{12}}(N_4 + N_5) - \sqrt{\frac{5}{12}}(N_7 + N_8)$	$= 0$		

$$\begin{array}{rcl}
 P_9 = \frac{1}{\sqrt{2}}(N_9 + N_{10}) & T = 0 & \\
 P_{10} = \frac{1}{\sqrt{2}}(N_9 - N_{10}) & = 1 & \\
 P_{11} = N_{11} & = 1 & \\
 P_{12} = N_{12} & = 1 & \\
 P_{13} = N_{13} & = 0 & 
 \end{array}
 \left. \vphantom{\begin{array}{rcl} P_9 \\ P_{10} \\ P_{11} \\ P_{12} \\ P_{13} \end{array}} \right\} \begin{array}{l} {}^3D_1 \\ {}^5P_1 \\ {}^5D_1 \end{array}$$

Some degeneracies occur as in previous cases. These permit a certain latitude in the linear combinations chosen. The ones selected above were chosen partly for symmetry reasons and partly to maximize the particle widths which are calculated in a following section.

#### B.4. $J = 0^+$ Wave Functions for $Be^8$

The ground state of  $Be^8$  has zero spin and even parity. From 1p shell single particle wave functions nine  $J = 0^+$  functions can be formed, three of which have the spectroscopic designation  ${}^1S_0$ , five are  ${}^3P_0$ , and one is  ${}^5D_0$ . It may be expected that the state of lowest energy will be among the  ${}^1S_0$  states. They are listed in Table 14.

Table 14

#### ${}^1S_0$ Wave Functions

	$L_N$	$S_N$	$L_P$	$S_P$	L	S	J	
$Q_1$	2	0	2	0	0	0	0	} ${}^1S_0$
$Q_2$	1	1	1	1	0	0	0	
$Q_3$	0	0	0	0	0	0	0	



Table 14 (continued)

$$Q_1 = \left[ \sqrt{\frac{1}{5}} y_2^2(n) y_2^2(p) - \sqrt{\frac{1}{5}} y_2^1(n) y_2^1(p) + \sqrt{\frac{1}{5}} y_2^0(n) y_2^0(p) - \sqrt{\frac{1}{5}} y_2^{\bar{1}}(n) y_2^{\bar{1}}(p) + \sqrt{\frac{1}{5}} y_2^{\bar{2}}(n) y_2^{\bar{2}}(p) \right] \chi_0^{\circ}(n) \chi_0^{\circ}(p)$$

$$Q_2 = \left[ \sqrt{\frac{1}{3}} y_1^1(n) y_1^1(p) - \sqrt{\frac{1}{3}} y_1^0(n) y_1^0(p) + \sqrt{\frac{1}{3}} y_1^{\bar{1}}(n) y_1^{\bar{1}}(p) \right] \left[ \sqrt{\frac{1}{3}} \chi_1^1(n) \chi_1^1(p) - \sqrt{\frac{1}{3}} \chi_1^0(n) \chi_1^0(p) + \sqrt{\frac{1}{3}} \chi_1^{\bar{1}}(n) \chi_1^{\bar{1}}(p) \right]$$

$$Q_3 = y_0^{\circ}(n) y_0^{\circ}(p) \chi_0^{\circ}(n) \chi_0^{\circ}(p)$$

The eigenfunctions of  $\mathcal{C}^2 = 2I - P_{13} - P_{23} - P_{14} - P_{24}$  are the following linear combinations of  $Q_1$ ,  $Q_2$ , and  $Q_3$  :

$$R_1 = \sqrt{\frac{5}{18}} Q_1 - \sqrt{\frac{4}{18}} Q_2 + \sqrt{\frac{9}{18}} Q_3 \quad T = 2$$

$$R_2 = \sqrt{\frac{5}{18}} Q_1 - \sqrt{\frac{4}{18}} Q_2 - \sqrt{\frac{9}{18}} Q_3 \quad = 0$$

$$R_3 = \sqrt{\frac{4}{9}} Q_1 + \sqrt{\frac{5}{9}} Q_3 \quad = 0$$

Since the ground state of  $\text{Be}^8$  has  $T = 0$  a choice must be made between  $R_2$  and  $R_3$  or some linear combination of them.  $R_3$  is chosen because the space part of its wave function is symmetric under the interchange of any pair of particles. If the major part of the forces between nucleons are of the Wigner and Majorana types this should make such space symmetric wave functions very low in energy.

### B.5. Channel Spin Wave Functions

The formulas for channel spin wave functions given in Table 7 for the  $jj$  coupling case apply here when the appropriate LS wave functions are used for  $\text{Li}^7$ . These are  $K_8$  and  $K_{13}$  for the ground state and first excited state, respectively.

### C. Radiative Decay Widths

One way of testing the merit of the wave functions obtained from the two coupling schemes is to compute from them radiative decay widths. In the preceding sections wave functions have been proposed for the ground state of  $\text{Be}^8$  and the excited states at 17.63 and 18.14 Mev. Using these wave functions the suggested computations will be made and compared with experiment.

The excited states have  $J = 1^+$  and the ground state  $J = 0^+$ , so the radiation must be magnetic dipole in character. The appropriate interaction Hamiltonian is then

$$\mathcal{H}'(M1) = i \frac{e}{2Mc} \sqrt{\frac{2\pi \hbar c^2}{\omega}} \underline{e} \times \underline{k} \cdot \left\{ \underline{L}_p + g_p \underline{S}_p + g_n \underline{S}_n \right\}.$$

The decay width is

$$\begin{aligned} \Gamma_\gamma &= 2\pi \int d\mathbf{p}_F \left| \langle f | \mathcal{H}' | i \rangle \right|^2 \\ &= 2\pi \frac{\omega^2}{(2\pi c)^3 \hbar} \int d\Omega_{\mathbf{k}} \sum_{\text{pol}} \left| \langle f | \mathcal{H}' | i \rangle \right|^2 \end{aligned}$$

The intensity of radiation from each of the three magnetic

substates of a  $J = 1^+$  level will be the same. The matrix elements themselves will be proportional to  $Y_1^M(\Omega)$ , so it will be convenient to average over the initial states. The integrant in the above formula will then be independent of angle so that the integral and sum over polarization can be done immediately :

$$\begin{aligned} \Gamma_\gamma &= 2\pi \frac{\omega^2}{(2\pi c)^3 \hbar} \cdot 4\pi \cdot 2 \cdot \frac{1}{3} \sum_{M=-1}^1 | \langle f | \mathcal{H}' | M \rangle |^2 \\ &= \frac{1}{3} \frac{e^2}{\hbar c} \left( \frac{\hbar \omega}{Mc^2} \right)^3 Mc^2 \Delta \end{aligned}$$

$$\Delta = \sum_{M=-1}^1 \left| \langle f | \frac{e \times k}{k} \cdot \left\{ \frac{1}{\hbar} (L_p + g_p S_p + g_n S_n) \right\} | M \rangle \right|^2$$

is a dimensionless quantity measuring the strength of the transition. The computation of  $\Delta$  is perfectly straight forward though, for the case of jj coupling, somewhat tedious.

The results of these computations are tabulated in Table 15. On the basis of arguments presented previously, the ground state wave functions used are  $G_1$  and  $R_3$  in the jj and LS coupling schemes respectively.

Table 15

Gamma Radiation Widths

1. jj Coupling

	$\Delta$	$\Gamma_\gamma$
$E_1$	$1/54 (2 + g_p - g_n)^2$	38 ev
$E_2$	0	0
$E_3$	$1/9 (1 - g_p + g_n)^2$	96
$E_4$	0	0
$E_5$	0	0
$E_6$	$1/9 (1 - g_p - g_n)^2$	1
$E_7$	0	0
$E_8$	0	0
$E_9$	0	0
$E_{10}$	0	0
$E_{11}$	0	0
$E_{12}$	0	0
$E_{13}$	0	0

Table 15 (continued)

2. LS Coupling

	$\Delta$	$\Gamma_\gamma$
P <sub>1</sub>	8/9	14 ev
P <sub>2</sub>	0	0
P <sub>3</sub>	$\frac{8}{27} (\epsilon_p - \epsilon_n)^2$	410
P <sub>4</sub>	0	0
P <sub>5</sub>	0	0
P <sub>6</sub>	0	0
P <sub>7</sub>	0	0
P <sub>8</sub>	0	0
P <sub>9</sub>	0	0
P <sub>10</sub>	0	0
P <sub>11</sub>	0	0
P <sub>12</sub>	0	0
P <sub>13</sub>	0	0

Comparison of these values with the experimental gamma widths will be postponed until a later section.

D. Particle Emission Widths.

The theory of resonance reactions developed by Wigner and his collaborators ( 14 ) leads to the following expression for particle emission widths :

$$\Gamma = 2kRv \cdot \frac{\hbar^2}{MR^2} \cdot \theta^2$$

In this expression  $kRv = kR (F_l^2 + G_l^2)^{-1}$  is the well known Coulomb penetration factor and

$$\theta^2 = \sum_l \left| \sqrt{\frac{R}{2}} \int_S X_l^* \phi_c \, dS \right|^2$$

is a dimensionless measure of  $\Gamma$  where  $X_l$  and  $\phi_c$  are the channel spin wave function and compound state wave function respectively.

The integral indicated is actually a sum of several integrals, each taken over the volume of all particles except the one being emitted and over the surface of this one. In our case, where either of two protons (particle numbers 3 and 4) may be emitted, the integral is

$$\int_{S_4} X_l^* \phi_c \, dv_1 dv_2 dv_3 dS_4 + \int_{S_3} X_l^* \phi_c \, dv_1 dv_2 dv_4 dS_3 .$$

The surfaces  $S_3$  and  $S_4$  separate the region, where the emitted particle interacts strongly with the others, from the region in which it feels at most Coulomb forces.

In the independent particle model the integrals can be resolved into two factors. One is essentially the square of the magnitude of the single particle radial wave function; the other is a statistical factor which is the value the integral would take if extended over

the entire configuration space. The factor depending on the radial wave function (designated by  $x_1$  in Tables 16 and 17) can be calculated if one assumes a definite potential well in which the particles move. These calculations have been made by Lane<sup>(9)</sup> for the case of a square well. As may be seen by consulting his curves, the value of this factor is not very sensitive to the factors which determine it. The suggested range of values is 0.6 to 1.4 for the 1p shell.

The statistical factor is a sum of contributions from the various channels. The ratios of these parts to one another are the well known channel spin ratios. These and the other relevant quantities are listed in Table 16 for elastic scattering and in Table 17 for inelastic scattering.

Table 16

	$\theta_1^2$	$\theta_2^2$	$\theta_1^2/\theta_2^2$	$\theta^2 = \theta_1^2 + \theta_2^2$	$\Gamma(440)$	$\Gamma(1030)$
jj Coupling						
$E_1$	$\frac{1}{9} x_1$	$\frac{1}{45} x_1$	5	$\frac{2}{15} x_1$	14 kev	100 kev
$E_2$	0	0	-	0	0	0
$E_3$	$\frac{1}{12} x_1$	$\frac{5}{12} x_1$	$\frac{1}{5}$	$\frac{1}{2} x_1$	50	360
$E_4$	0	0	-	0	0	0
$E_5$	0	0	-	0	0	0
$E_6$	$\frac{1}{12} x_1$	$\frac{5}{12} x_1$	$\frac{1}{5}$	$\frac{1}{2} x_1$	50	360

Table 16 (continued)

	$\theta_1^2$	$\theta_2^2$	$\theta_1^2/\theta_2^2$	$\theta^2 = \theta_1^2 + \theta_2^2$	$\Gamma(440)$	$\Gamma(1030)$
E <sub>7</sub>	0	0	-	0	0	0
E <sub>8</sub>	0	0	-	0	0	0
E <sub>9</sub>	0	0	-	0	0	0
E <sub>10</sub>	0	0	-	0	0	0
E <sub>11</sub>	0	0	-	0	0	0
E <sub>12</sub>	0	0	-	0	0	0
E <sub>13</sub>	0	0	-	0	0	0

LS Coupling

P <sub>1</sub>	$\frac{4}{9} x_1$	0		$\frac{4}{9} x_1$	45 kev	320 kev
P <sub>2</sub>	0	0	-	0	0	0
P <sub>3</sub>	0	0	-	0	0	0
P <sub>4</sub>	0	0	-	0	0	0
P <sub>5</sub>	0	0	-	0	0	0
P <sub>6</sub>	$\frac{1}{18} x_1$	$\frac{5}{18} x_1$	$\frac{1}{5}$	$\frac{1}{3} x_1$	33	240
P <sub>7</sub>	0	0	-	0	0	0
P <sub>8</sub>	$\frac{1}{18} x_1$	$\frac{5}{18} x_1$	$\frac{1}{5}$	$\frac{1}{3} x_1$	33	240
P <sub>9</sub>	$\frac{1}{36} x_1$	$\frac{1}{180} x_1$	5	$\frac{1}{30} x_1$	3.3	24
P <sub>10</sub>	$\frac{1}{36} x_1$	$\frac{1}{180} x_1$	5	$\frac{1}{30} x_1$	3.3	24



Table 16 (continued)

	$\theta_1^2$	$\theta_2^2$	$\theta_1^2/\theta_2^2$	$\theta^2 = \theta_1^2 + \theta_2^2$	$\Gamma(440)$	$\Gamma(1030)$
P <sub>11</sub>	0	0	-	0	0	0
P <sub>12</sub>	0	0	-	0	0	0
P <sub>13</sub>	0	0	-	0	0	0

Table 17

Inelastic Scattering Widths

	$\theta_1^2$	$\theta_0^2$	$\theta_0^2/\theta_1^2$	$\theta^2 = \theta_0^2 + \theta_1^2$	$\Gamma$
	1. jj Coupling				
E <sub>1</sub>	$\frac{1}{3} x_1$	$\frac{1}{6} x_1$	$\frac{1}{2}$	$\frac{1}{2} x_1$	64 kev
E <sub>2</sub>	0	0	-		0
E <sub>3</sub>	0	0	-		0
E <sub>4</sub>	$\frac{1}{6} x_1$	$\frac{1}{3} x_1$	2	$\frac{1}{2} x_1$	64
E <sub>5</sub>	0	0	-	0	0
E <sub>6</sub>	0	0	-	0	0
E <sub>7</sub>	$\frac{1}{6} x_1$	$\frac{1}{3} x_1$	2	$\frac{1}{2} x_1$	64
E <sub>8</sub>	0	0	-	0	0
E <sub>9</sub>	0	0	-	0	0
E <sub>10</sub>	0	0	-	0	0
E <sub>11</sub>	0	0	-	0	0
E <sub>12</sub>	0	0	-	0	0
E <sub>13</sub>	0	0	-	0	0

Table 17 (continued)

	$\theta_1^2$	$\theta_0^2$	$\theta_0^2/\theta_1^2$	$\theta^2 = \theta_0^2 + \theta_1^2$	$\Gamma$
2. LS Coupling					
$P_1$	$\frac{2}{9} x_1$	0	0	$\frac{2}{9} x_1$	28 kev
$P_2$	0	0	-	0	0
$P_3$	0	0	-	0	0
$P_4$	0	0	-	0	0
$P_5$	0	0	-	0	0
$P_6$	$\frac{1}{9} x_1$	$\frac{2}{9} x_1$	2	$\frac{1}{3} x_1$	42
$P_7$	0	0	-	0	0
$P_8$	$\frac{1}{9} x_1$	$\frac{2}{9} x_1$	2	$\frac{1}{3} x_1$	42
$P_9$	$\frac{1}{18} x_1$	$\frac{1}{9} x_1$	2	$\frac{1}{6} x_1$	21
$P_{10}$	$\frac{1}{18} x_1$	$\frac{1}{9} x_1$	2	$\frac{1}{6} x_1$	21
$P_{11}$	0	0	-	0	0
$P_{12}$	0	0	-	0	0
$P_{13}$	0	0	-	0	0

E. Discussion of Level Parameters

The experimental data which we wish to discuss are listed in Table 18.

Table 18

<p>440 kev</p> <p>T = 1</p> <p><math>\alpha_1^2/\alpha_2^2 = 1/5</math></p> <p><math>\Gamma_p = 14</math> kev</p> <p><math>\Gamma_\gamma = 22</math> ev</p> <hr style="width: 10%; margin-left: 0;"/>	<p>1030 kev</p> <p>T = 0</p> <p><math>\alpha_1^2/\alpha_2^2 = 1/5</math></p> <p><math>\Gamma_p = 200</math> kev</p> <p><math>\Gamma_\gamma &lt; 6</math> ev</p> <p><math>\Gamma_{p'} = 9</math> kev</p>
---	---

Referring now to Table 16 where the elastic scattering widths are given, it may be seen that both the LS and jj coupling schemes give two states - one having T = 1 and the other T = 0 - with the correct channel spin ratios ( $\alpha_1^2/\alpha_2^2 = \theta_1^2/\theta_2^2$ ). They are respectively  $E_3$  and  $E_6$  for jj coupling and  $P_6$  and  $P_8$  for LS coupling. This is most encouraging for it offers an "explanation" of what would otherwise have seemed quite odd, namely that the channel spin ratio happened to be just that value which resulted in isotropic angular distributions. The explanation, of course, in either case is that there is an additional quantum number besides total angular momentum and isotopic spin which fixes the angular distribution. In the case of jj coupling it is the configuration, i.e. the number of particles in each of the  $p_{3/2}$  and  $p_{1/2}$  subshells, and in the case

of LS coupling it is orbital and spin angular momenta.

The elastic scattering widths corresponding to these same wave functions are larger than the experimental widths by factors up to four, but this can be explained away.  $x_1$ , which depends on the value of the radial wave functions at the surface of the nucleus, could be less than the value used by a factor of two or even three. Lane<sup>(9)</sup> is inclined to favour smaller values for  $x_1$  as he finds that a harmonic oscillator potential gives a smaller value than the square well, and it is generally believed that the rounded bottom of an oscillator potential is more realistic. Also - from the point of view taken here - it is perfectly permissible to take linear combinations of wave functions having the same quantum numbers, as we have no a priori reasons for favouring the particular linear combinations chosen here other than the esthetic one that the present ones display certain symmetries in their construction. We will come back a little later to the question of using such linear combinations.

The radiation widths, computed for the jj and LS wave functions that seem to be indicated by the elastic scattering, are both zero for the LS case and 96 and 1 ev for the 440 and 1030 kev levels in the jj coupling scheme. In the case of LS coupling, the existence of such a large width as 410 ev for  $P_3$  (when compared with the experimental values of 22 and  $< 6$  ev) makes it plausible that small impurities in the wave function of either the ground state or the excited state, or more likely both, could be responsible for the observed widths. In the jj case the same argument can be applied to the 1030 kev state for which  $E_0$  predicts  $\Gamma_\gamma = 1$  ev while the observed value is  $< 6$  ev. The figure of 6 ev for the 1030 kev resonance is the

combined radiation width for transitions to the ground state and first excited state of  $\text{Be}^8$  which have not been resolved. It could be that most of the resonant radiation goes to the first excited state of  $\text{Be}^8$  so that this argument is not needed. In the case of the 440 kev state, the predicted value of 96 ev is greater than the observed value of 22 ev by about the same factor that is found in the case of the elastic scattering widths. This suggests that the device of taking a linear combination of, say,  $E_3$  and  $E_4$  would make possible the fitting of all the data for the 440 kev resonance.

Finally we come to the inelastic scattering. If the LS wave function  $P_6$  is used, a width of 42 kev is predicted while the observed value is about 9 kev. The value of 42 kev can be reduced by the same devices suggested in the case of elastic scattering. However, such methods must be applied uniformly to the elastic and inelastic scattering and none of them will change the ratio of the predicted widths. This is  $\Gamma_{p'}/\Gamma \simeq 0.17$  while the observed ratio is  $\Gamma_{p'}/\Gamma \simeq 0.045$ . The jj wave functions offer more flexibility, as the ratio  $\Gamma_{p'}/\Gamma$  can be adjusted arbitrarily by taking a linear combination of  $E_6$  and  $E_7$ .

In surveying the above discussion we see that neither coupling scheme is at odds with the observed data.

However, neither will account in a straight forward manner for more than the channel spin ratio and the approximate values of the elastic scattering widths. If a choice had to be made on the basis of the data presented, the jj coupling scheme would seem to have the edge.

Of late a number of "intermediate coupling" calculations have been made on a few of the light nuclei.<sup>(15 - 18)</sup> The success of these

in giving a number of particle and radiation widths in fair agreement with observation raises hopes that the same might be accomplished in the case of  $\text{Be}^8$ . There is one reason for being less optimistic here. That is that probably such a computation would not give the channel spin ratio  $\alpha_1^2 / \alpha_2^2 = 1/5$  which is obtained in the limiting cases of pure LS or jj coupling. A deviation outside the limits of  $1/6 < \alpha_1^2 / \alpha_2^2 < 1/4$  would certainly be incompatible with the angular distribution of gamma rays at the peak of the 440 kev resonance, and probably not much more of a deviation from  $\alpha_1^2 / \alpha_2^2 = 1/5$  could be tolerated if the angular distribution of the inelastic scattering at the 1030 kev resonance is to be fitted. Such an intermediate coupling computation should be undertaken for just this point - whether or not a reasonable value of the channel spin ratio can be obtained - may offer a fairly critical test of its assumptions.

REFERENCES

- (1) Devons, S. and M.G.N. Hine, Proc. Roy. Soc. 199A, 56 (1949).
- (2) Devons, S. and M.G.N. Hine, Proc. Roy. Soc. 199A, 73 (1949).
- (3) Walker, R.L. and B.D. McDaniel, Phys. Rev. 74, 315 (1948).
- (4) Nabholz, Stoll, and Wäffler, Helv. Phys. Acta 25, 701 (1952).
- (5) Blatt, J.M. and V.F. Weisskopf, Theoretical Nuclear Physics, John Wiley & Sons, New York.
- (6) Fowler, Lauritsen, and Lauritsen, Phys. Rev. 73, 181 (1948).
- (7) Cohen, E.R., Ph.D. Thesis, California Institute of Technology (1949).
- (8) Warters, Fowler, and Lauritsen, Phys. Rev. 91, 917 (1953).
- (9) Lane, A.M., The Reduced Widths of Nuclear Energy Levels, AERE T/R 1289.
- (10) Kraus, A.A., Phys. Rev. 93, 1308 (1954).
- (11) Mozer, Fowler, and Lauritsen, Phys. Rev. 93, 829 (1954).
- (12) Haxel, Jensen, and Suess, Phys. Rev. 75, 1766 (1949).
- (13) Mayer, M.G., Phys. Rev. 75, 1969 (1949).
- (14) Wigner, E.P. and L. Eisenbud, Phys. Rev. 72, 29 (1947).
- (15) Lane, A.M., Proc. Phys. Soc. A 66, 977 (1953).
- (16) Lane, A.M. and L.A. Radicati, Proc. Phys. Soc. A 67, 167 (1954).
- (17) Lane, A.M., Proc. Phys. Soc. A 68, 189 (1955).
- (18) Lane, A.M., Proc. Phys. Soc. A 68, 189 (1955).